A thesis report on

CLOSED–LOOP CONTROL FOR VIBRATION SUPPRESION OF A SINGLE–LINK FLEXIBLE MANIPULATOR USING COMMAND SHAPING TECHNIQUES

Submitted in the partial fulfilment of the requirement for

the award of the degree of

MASTER OF ENGINEERING

IN

CAD/CAM & ROBOTICS

Submitted by

Aashish Gupta

Roll No.: 801181005

Under the guidance of

Dr. Ashish Singla

Assistant Professor

Mechanical Engineering Department

Thapar University, Patiala.

MECHANICAL ENGINEERING DEPARTMENT

Thapar University, Patiala

July 2013

Certificate

I hereby certify that the thesis entitled "**CLOSED-LOOP CONTROL FOR VIBRATION SUPPRESION OF A SINGLE-LINK FLEXIBLE MANIPULATOR USING COMMAND SHAPING TECHNIQUES**" is an authentic record of my own work carried out in partial fulfillment of the requirement for the award of degree of **Master of Engineering** in **CAD/CAM & Robotics** under the guidance of **Dr. Ashish Singla**, Assistant Professor, MED, Thapar University, Patiala.

Aashish Gupta

Aashish Gupta

801181005

This is to certify that the above statement made by the candidate is correct and true to the best of my knowledge.

Dr. Ashish Singla
Assistant Professor
Mechanical Engineering Department
Thapar University, Patiala

Countersigned By:-

Dr. S. K. Mohapatra
Senior Professor and Dean of Academic Affairs
Mechanical Engineering Department
Thapar University, Patiala

Dr. Ajay Batish
Professor and Head
Mechanical Engineering Department
Thapar University, Patiala

Acknowledgement

Though only my name appears on the cover of this thesis, a lot of people have contributed to its completion. I owe my gratitude to all those people who have made this dissertation possible and because of whom my post graduate experience has been one that I will cherish forever.

My deepest gratitude is to my supervisor **Dr. Ashish Singla**. I have been amazingly fortunate to have an advisor who gave me the freedom to explore on my own and at the same time the guidance to recover when my steps faltered. He taught me how to question thoughts and express ideas. His patience and support helped me overcome many crisis situations and finish this dissertation. I am grateful to him for holding me to high research standards and enforcing strict validations for each research result and thus teaching me how to do research.

I am also thankful to all the staff members of mechanical engineering department who are directly or indirectly concerned within the completion of my thesis.

Many friends have helped me stay sane through these years. Their support and care helped me overcome setbacks and keep me centered on my study. I greatly worth their friendship and I deeply appreciate their belief in me.

Most significantly, none of this would have been possible without the love and patience of my family. My family to whom this dissertation is dedicated to, has been a relentless supply of love, concern, support and strength of these years. I would like to express my heart – felt gratitude to my family particularly my elder brother for his support.

Aashish Gupta

Abstract

In today's fast growing world, the motivation to utilize robotic manipulators has also been actuated by the needs and demand of the industrial automation. Most of the existing manipulators were designed with maximum stiffness in order to minimize the vibrations induced within the manipulator and also to maintain the required positional accuracy. This high stiffness is achieved by using heavy materials and bulky design, which require high power consumption and have reduced speed of operations, the downside in conventional manipulators. That is where the need of flexible manipulators arise and attention is focused more towards the flexible manipulators than rigid manipulators owing to various advantages like small actuators, reduced inertia, high mobility, less power consumption, greater payload-to-robot-weight ratio, larger work volumes of such manipulators. However, how to handle structural vibrations, which are inherent with flexible manipulators, is a challenging task both in the modeling and control phase. Various research methodologies has been developed by researchers to cope with vibrations of flexible systems.

In this thesis, a theoretical investigation is presented for dynamic modeling as well as vibration suppression of a single-link flexible manipulator. A mathematical model is developed on the basis of finite element method considering flexibility, inertia and damping effects in nature. The developed dynamic model is validated by comparing the results with published literature. As structural vibrations are inherent with flexible manipulators, the concept of command shaping has been utilized to minimize the vibrations. Moreover, a hybrid controller is developed, which is a combination of linear feedback control and input shaping. Simulation results on a single-link flexible manipulator demonstrate the efficacy of the proposed controller in achieving the positioned accuracy and reducing the vibration levels.

Contents

List of Figures

List of Tables

List of Symbols

θ(t)	Angular displacement
ϕ_i	Hermite shape functions
ρ	Density
E	Modulus of elasticity
I	Area moment of inertia
l	Length
f	Force
I_{hub}	Hub inertia
ω	Frequency in radian
ω_n	Natural frequency
ω_d	Damped Frequency
t_i	Time impulse
A_i	Amplitude of impulse
M_n	Elemental mass matrix
K_n	Elemental stiffness matrix
g	Acceleration due to gravity
ζ	Damping ratio
t	Time
K	Gain of the system
K_P	Proportional gain
K_V	Derivative gain
A_c	Linear gain of the amplifier
K_d	Controller gain matrix
K_n	Controller gain matrix

CHAPTER 1 INTRODUCTION

1.1 Conventional Manipulators

Robotic manipulators serve an excellent purpose in accomplishing dangerous, monotonous, and tedious jobs. For most of the existing conventional manipulators, stiffness has invariably been a vital issue. Mostly manipulators are designed to maximize stiffness in an effort to minimize the vibration of the end-effector to achieve good position accuracy. Heavy material and large designs of manipulator are used to achieve high stiffness. Hence, the prevailing rigid manipulators are shown to be inefficient in terms of power consumption or speed with relation to the operative payload. Also, the operation of high precision robots is severely restricted by their dynamic deflection that persists for an amount of time after a move is completed. The settling time required for these vibrations delays the operations effecting the production in industries. Thus, high speed and high accuracy are conflicting factors during accomplishment of a task by a robot efficiently. Several industrial manipulators used to face the problem of arm vibrations during high speed motion.

In order to improve industrial productivity, it is needed to scale back the load of the arms to enhance their speed of operation. For these purposes, it is very desirable to build flexible robotic manipulators. Compared to the traditional heavy and bulky robots, flexible link manipulators have the potential advantage of lower cost value, larger work volume and operational speed, greater payload-to-manipulator-weight quantitative relation, smaller actuators, lower energy consumption, higher mobility, better transportability and safer operation owing to reduced inertia. However, the greatest disadvantage of these manipulators is the vibration owing to their low stiffness

Powerful and large robotic manipulators are required in nuclear maintenance, e.g., to perform decontamination tasks. The nozzle dam positioning task for maintenance of a nuclear power plant steam generator needs a robust manipulator with terribly fine absolute positioning accuracy.

1.2 Flexible Manipulators

To overcome the drawbacks of industrial robots existing today of huge weights, high energy consumptions and low speed operations, much research has been carried out in modeling and control of lightweight flexible manipulators.

Flexibility in a flexible manipulator means the thickness or width of the link is very small compared with the height of the link resulting in high deflection in the link. Flexible manipulator systems are receiving considerable attention because of their benefits over standard robot manipulators. It's because of their quicker response, lower energy consumption, comparatively smaller actuators, higher payload to weight quantitative relation and less overall cost. However, because of their flexible nature, induced vibrations seem within the system throughout and after a positioning maneuvering. To formulate and implement an effective and economical control strategy for efficient vibration suppression in the system, it's vital to recognise the flexible nature of the manipulator and construct a mathematical model for the system that accounts for the interactions with actuators and payload.

1.3 Importance of Flexible Manipulators

There are various reasons for development of the flexible robot mechanical structure. One of the reason is light weight of flexible manipulators and cost reduction but other benefits are lower power consumption, improved dexterity, safety issues and lower environmental impact, high path accuracy, high speed accuracy, high speed and acceleration in discrete applications, small settling times, etc. Light weight of the flexible manipulator results in reduced system inertia.

1.4 Challenges in Flexible Manipulators

1. Controlling vibration of flexible manipulator having large degree of freedom.
2. Modeling a complex flexible structure.
3. For very flexible structures, achieve high performance control.
4. Controlling structure where non-linear and complex dynamics is involved.
5. Dealing with unknown parameters in the system.

1.5 Applications

1. **Space robots:** In the recent years of flexible manipulators, the study on the control of a flexible arm manipulator started as a part of the space robots research, as shown in Fig. 1.1. The objective in space flexible manipulator is to reduce weight of space manipulator to make it as light as possible which allows the scientists to reduce the launching thrust.

Fig. 1.1: Flexible manipulators in space applications [1].

2. **Nuclear maintenance:** In the nuclear power plants, due to access restriction of floor space, flexible manipulators are required to perform risky tasks like decontamination task etc., as shown in Fig. 1.2. The nozzle dam positioning task for maintenance of a nuclear power plant steam generator requires a flexible manipulator robot with very fine absolute positioning accuracy.

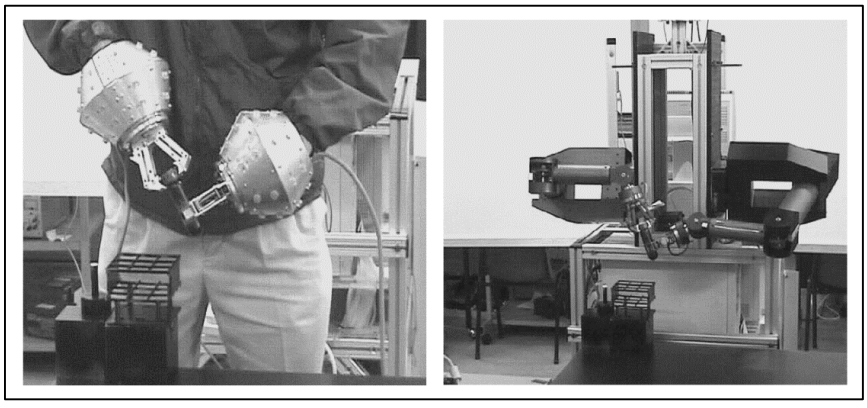

Fig. 1.2: Flexible manipulators in nuclear maintenance [2].

3. **Micro surgical operations:** In microsurgery, flexible manipulators are used for deep and narrow sites of the body are currently the most difficult areas to perform surgery. Typical examples are neurosurgery, head and neck surgery and microsurgery and an area that is not accessible with an endoscope through the mouth, as shown in Fig. 1.3.

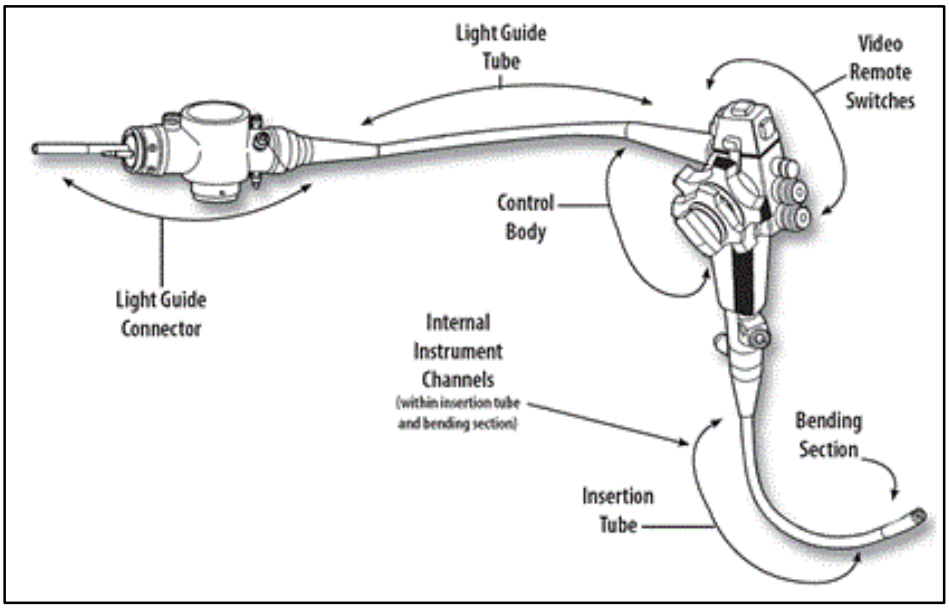

Fig. 1.3: Flexible endoscope [3].

4. **Other field applications:** Flexible manipulators can also be used in grinding, painting or drawing, pattern recognition with soft touching etc. A flexible manipulator used for drilling is shown in Fig. 1.4.

Fig. 1.4: Flexible manipulators in industrial applications [1].

1.6 Scope of the Thesis

In this thesis, main focus has been laid on the dynamic modeling and vibration suppression of the flexible manipulators. A detailed literature has been done on the dynamic modeling of the flexible manipulators and the control techniques for suppressing the vibrations of the manipulator to achieve high end-effector positional accuracy. In this thesis, first the mathematical model is developed for a single-link flexible manipulator. The resonance frequencies are calculated and compared with literature published for validation. Validation is important because shaping is very sensitive to modeling uncertainties, the performance of the shaper depends highly on the accuracy of the mathematical model. So, it is important to validate the model in terms of natural frequencies and damping ratios of the system. Then, command shaping is used for improving the settling time and positional accuracy for minimizing residual vibration of the flexible manipulator. In command shaping, a command signal is used that cancels its own vibration. It means vibration caused by first command signal is canceled by vibration caused second command signal. Then, a closed-loop linear feedback controller is developed for positional accuracy and vibration a command suppression. The PD controller is implemented on the dynamic model and vibrations are suppressed for positional accuracy of the flexible manipulator.

1.7 Organisation of the Thesis

In Chapter 1, the introduction to conventional and flexible manipulator considering various aspects is presented. It consists of the need of light weight manipulators developed in respect to the disadvantages of the conventional manipulators. The various challenges occur to model and control of the flexible manipulator and the applications of the flexible manipulator in space, nuclear technology, etc. are also briefed.

In Chapter 2, the literature related to the flexible manipulators is presented. Various researchers gave their contribution in the development of flexible manipulators. The theoretical model as well as experimental setup of single and multilink flexible manipulators developed by researchers across the world is presented briefly.

In Chapter 3, the modeling techniques used for the flexible manipulators are discussed. In this Chapter, the dynamic model of a single-link flexible manipulator is developed mathematically using finite element method. It is important to validate the model because of high sensitivity of input shaping to the uncertainties in the mathematical model and performance of shaper is dependent on accuracy of mathematical model. Hence, the model is validated in terms of damping ratios and natural frequencies. In this Chapter, the resonant frequencies are calculated and compared with the published literature.

In Chapter 4, the concept of command shaping for vibration suppression of flexible manipulators is presented. The basis of input shaping as well as the analytical formulation of the shaper is discussed. Moreover, to achieve high positional accuracy, a linear state feedback control scheme i.e. a proportional derivative control scheme is discussed.

In Chapter 5, results are obtained and graphs are plotted for vibration suppression of the flexible manipulator using a control scheme and simulation results of the flexible manipulator are carried out to demonstrate the vibration levels. A hybrid controller which is a combination of feedback control and command shaping is developed. The results are carried out in MATLAB environment.

In Chapter 6, results are summarized and future directions for the dynamic modeling and control of flexible manipulators are mentioned.

CHAPTER 2 LITERATURE REVIEW

2.1 Introduction

Due to the importance and usefulness of these topics, researchers worldwide are now a day engaged in the investigation of dynamics and control of flexible manipulators. In the following literature, various modeling, controlling and application aspects of flexible manipulators of the past are presented.

2.2 Literature Review

Nicosia et al. [2] presented a dynamic model, which was obtained by generalized Lagrangian approach with motion equations and to control the model, general properties of the models were investigated with the help of SAM Language. A single link rotating robot arm and double link robot arm with revolute joints is used to explain the method used in literature as an application. The process could sometime lead to complex and time consuming results. Investigation in the possibility of using a linearized version of motion equations can be done for deriving simpler control law even if it is valid just near the desired trajectory.

Hastings and Book [3] presented a modeling process to generate a linear state-space model for a single-link flexible manipulator consisting of a flexible arm with payload, DC torque motor, signal conditioning with analog to digital conversion for data acquisition, 16-bit computer system for implementation of control algorithms and digital to analog conversion for torque signal output. The model eigenvalues were matched with experimentally determined frequencies of the vibratory modes. Results showed that the actual damping responses tend to damp out faster than prediction, indicating increased damping of the vibratory modes occurring during large manipulator motions.

Wayne [4] presented a theoretical procedure for the mathematical representations commonly used in modeling flexible arms and arms with flexible drives. Modeling of flexible manipulator using Bernoulli-Euler beam equation, factors responsible for the design of the flexible arms, the

controlling the joints of flexible arms using advanced control algorithms, trajectory planning and trajectory tracking conditions are discussed. The flexible nature of the arm like nonlinear arms, controls of joints and tip motion were discussed. Result showed that more than one link flexible manipulator should be practically develop for better understanding in applications of flexible manipulators and to accompany the theoretical and simulation results to keep realism in the research.

Kenneth and Stephen [5] presented analysis and experimentation for a two-link flexible manipulator for vibration control with point to point movements assuming fixed reference frame to base for end position accuracy. Input control schemes (open loop compensator) was used for controlling such that impulse responses are superimposed to eliminate the last impulse. A two stage control scheme was adopted in which small motions were considered separate from large motions. Actuator input large angle movement and then endpoint acceleration feedback method was implemented for vibration suppression at end points of the links. Analysis results showed that joining the two stages of the control had developed the composite strategy, which is good for fast response capabilities of the input shaping with minimal residual vibrations as well as disturbance rejection.

Biswas and Klafter [6] presented a methodology for developing a mathematical model and control of flexible manipulator of a single-axis robot of simple geometry coupled system of ordinary and partial differential equations assuming no motion of arm in vertical plane and no longitudinal elongation in the link. A control methodology was presented to achieve a desired angular rotation of link in specified time and suppressing system vibrations simultaneously. Numerical results showed large reduction of oscillations during motion and improvement in the positioning accuracy of end effector at end of angular rotation of the flexible arm.

Mehrdad and Stanislaw [7] proposed a model with finite element approach for modeling equations of motions of lightweight spatial manipulator whose constraint equations describing relations between each link were added to equations of motion. The Lagrangian/Finite element approach was used to model the dynamics and takes into account the coupling effects between rigid body motion and the elastic deformations of the links and interaction between flexible links

and joint. Model was validated and effect of link and joint flexibilities were illustrated. The result of model showed that torsional deflections have more significant effect than bending deflections and joint transformations. Also, the effect of joint flexibility was significant when links were flexible too.

Everett and Compere [8] demonstrated how to design a two–dimensional flexible manipulator so that its fundamental vibration frequency was nearly independent of the rigid body position of the links. So that it act as rigid manipulator at its first natural frequency. Literature pointed that rather than designing a controller that handles a complex system, one might build a flexible manipulator that exhibits simpler dynamic behaviour than current designs.

Rosado and Yuhara [9] presented the mathematical modeling of two link flexible links of robotic manipulator with two flexible links and revolute joints using Newton-Euler formulation and the finite element method to derive the motion of equations, as shown in Fig. 2.1. They presented that PD controller parameters were adjusted relative to the arm flexibility to describe the effects of flexibility which limits the system stability, operational accuracy and control gains.

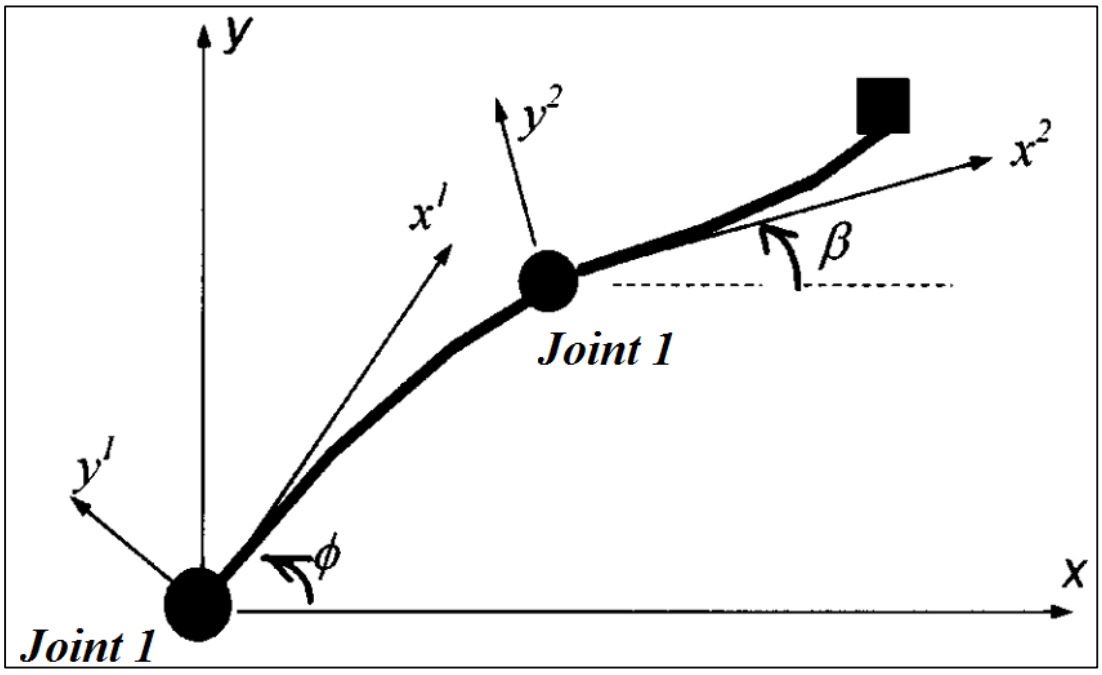

Fig. 2.1: Configuration of a two-link flexible robotic manipulator [9].

Rosado [10] presented a dynamic model for the design and control of a flexible robotic manipulator having two flexible links and two revolute joints in horizontal plane. The equations of motion were developed with Newton-Euler formulation and finite element method which represents the large motions, small motions, and their interactions in the manipulators. The dynamic equations obtained were utilized to discretize the displacements and computer simulation showed vibration suppression using PD feedback controller. Simulation result showed that sampling rate is affected by the flexibility, but still a real time control of the flexible manipulator possible.

Wen Chen [11] presented a linearized dynamic model for multi-link planar flexible manipulators with arbitrary number of flexible links, as shown in Fig. 2.2. The assumed mode method for modeling elastic deformation of each link considering each link as Euler Bernoulli beams and Lagrange approach was used for making dynamic equations of system. Rotary inertia and shear deformation were neglected. Numerical simulations were shown to verify the proposed method. Literature suggests that inverse dynamics could be used to find driving torque that excites least flexible deformation.

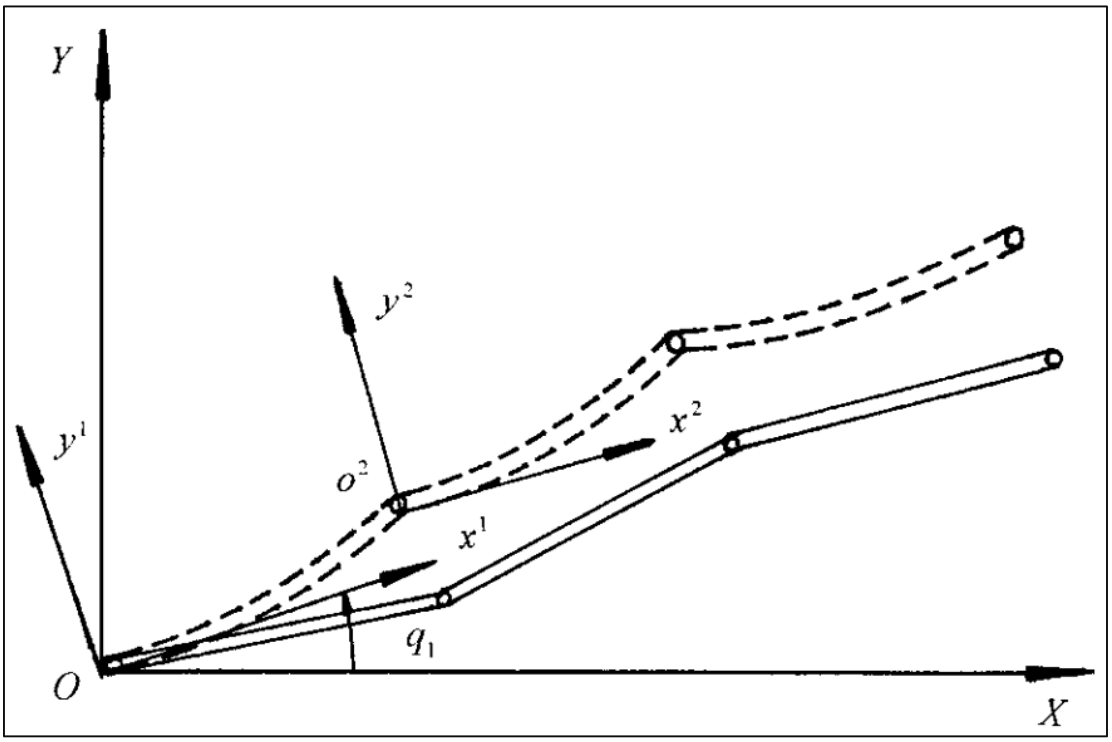

Fig. 2.2: Schematic of a planar multi-link flexible manipulator [11].

Tokhi et al. [12] presented theoretical and experimental investigations into the dynamic modeling and characterisation of a constrained planar single link flexible manipulator system. The equation of motions were developed using finite element methods considering inertia effects and structural damping. The developed model results were compared with an experimental test rig. Experimental results were presented for validation of the designed finite element model in time and frequency domain. The results show close agreement between simulated and experimental time responses and resonance frequencies of the system.

Mohamed and Tokhi [13] presented experimental investigations into the development of feed forward control strategies for vibration control of a flexible manipulator a laboratory scale apparatus using command shaping techniques based on input shaping and low pass and band stop filtering shown in Fig. 2.3. Performance of the technique was evaluated in terms of level of vibration reduction, time responses, robustness and processing times. Results showed that low-pass filtered input perform better than the band-stop filtered input. However, the processing time in developing an input shaping command was found longer as compared to that required or a filtered input.

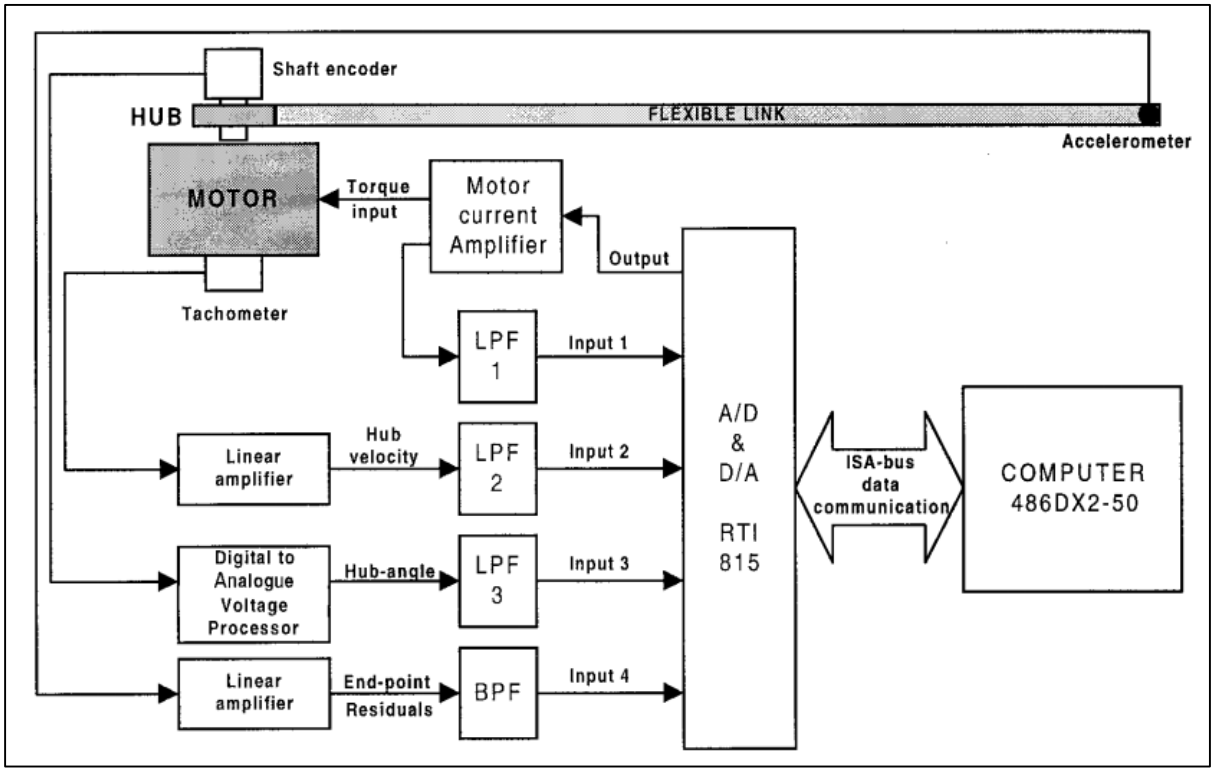

Fig. 2.3: Schematic diagram of the experimental flexible manipulator [13].

Martins et al. [14] presented a dynamic model of flexible manipulator based on assumed mode method considering linear as well as quadratic displacements and the finite element methodology.

Slow and fast trajectories are used for investigating the effect of the centrifugal forces. Two aspects of these systems the displacement amplitude and joint friction on IST manipulator (as shown in Fig. 2.4) and Sheffield manipulator are discussed briefly. Results showed that AMM with quadratic-displacement yields better results with hub-angle and FEM method yields better results with hub-velocity and end point acceleration.

Fig. 2.4: The IST manipulator [14].

Dwivedy and Eberhard [15] presented a literature survey to dynamic analyses of flexible robotic manipulators has been carried out till that time. Both link and joint flexibility were considered and an effort has been made to critically examine the methods used, their advantages and shortcomings and possible extension of these methods to be applied to general class of

problems. The literature for manipulator revealed that dynamic analysis and control of flexible manipulator is an emerging area in various fields. So reinvestigation needed in modeling techniques for large deformations and coupling of bending-bending, bending-torsion in the links. The literature shows that models used in flexible manipulators cannot take moderately large elastic deflections and also study of flexible manipulators is limited to single-link only. Paper involves different modeling technique literature with different number of links in the manipulator suggesting more effort in development of manipulator with low energy requirement.

Zain et al. [16] presented an investigation for performance of an intelligent hybrid iterative learning control scheme with input shaping for input tracking and end-point vibration suppression of the manipulator. The dynamic model of the system was derived with FEM and a collocated PD controller utilizing hub-angle and hub-velocity feedback was developed for control of rigid-body motion of system. Simulation and results of the flexible manipulator were presented in time and frequency domains. The control scheme implemented in literature and tested within simulation environment of a single-link manipulator without and with a payload.

Singhose [17] presented an investigation in literature of command shaping research since it was first proposed in the late 1950's. Literature consists of early command shaping methods and different current control techniques for increasing the robustness of the flexible manipulators. The dynamic mathematical models generally only estimates the natural frequencies and damping ratios. Command shaping is advantageous in various types of constraints like actuator limits, fuel usage and transient deflection limits, etc. which can become the part of design of commands and the merits of command shaping can be implemented machines throughout the world.

2.3 Observations from Literature Review

1. From literature, it is observed that most of the literature and research work is accomplished for flexible manipulator using feedforward techniques. Feedback control techniques for flexible manipulator are used rarely in the literature.
2. It is also observed that modeling of flexible manipulator is preferred with discrete systems rather than distributed system because of limitation of finding exact solution using distributed system.

3. It is observed from the literature that a flexible manipulator system can be discretized using three methods *i.e.* Assumed Mode Method, Lumped Parameter Method and Finite Element Method. The FEM method is generally preferred.
4. A flexible model cannot take care of moderately large elastic deflections. Therefore, reinvestigation of modeling and controlling techniques for large deformations, coupling of different bending and torsion modes in links is required.

CHAPTER 3 DYNAMIC MODELING OF FLEXIBLE MANIPULATORS

3.1 Introduction

The first step in design, analysis and control of the flexible manipulator is accurate dynamic mathematical modeling. A lot of models linear, nonlinear, numerical, analytical have been proposed in the literature. In this Chapter, various types of modeling techniques are discussed. One of the technique is used in modeling of a flexible manipulator. Later, the model is validated with published literature because the input shaping is sensitive to uncertainties in modeling and the shaper performance depends on modeling accuracy. Therefore, it is important to validate the model in terms of natural frequencies and damping ratios of the system.

3.2 Modeling of Flexible Manipulator

Modeling of flexible manipulators involves mathematical models of manipulators. The link flexibility must be considered in modeling of lightweight manipulators. However, due to the complexity of the link deformation, accurate modeling of flexible manipulators pose a challenge in practical design. The modeling techniques for flexible manipulators can be divided into two main parts as discussed below.

3.2.1 Distributed System

In distributed system, the flexible manipulator is a continuous nonlinear system described by partial differential equations, PDEs and with infinite number of degrees of freedom. An infinite dimensional model is not realistic to use in real applications as it imposes severe constraints on the design of controllers.

3.2.2 Discrete System

A finite dimensional model with the minimum number of parameters for the required accuracy level is generally preferred. The three levels of discrete modeling methods are:

(a) Finite Element Method

These models are the most accurate models. FEM models are widely used in the mechanical design of robot manipulators. Finite element method is an approximate solution method which often is used to solve complex systems. The finite element method is a powerful numerical solution technique that is used to solve vibration problems with complicating factors. Many of these factors are the result of complex geometries, non-uniform mass or stiffness distributions, and material or geometric nonlinearities.

(b) Lumped Parameter Method

The two basic assumptions in this method are that all objects are rigid bodies and all interactions between rigid bodies take place by kinematic joints. With this approach, a link can be divided into a number of rigid bodies connected by non-actuated joints. While lumped-parameter methods can be extended to more complicated systems, they are best suited for systems with chain-like geometries.

(c) Assumed Mode Method

These models are derived from the PDE formulation by modal truncation in terms of spatial mode eigen functions and time varying mode amplitudes. There are several ways to choose link boundary conditions and mode eigen function in this method. However, it is difficult with multi-links manipulators to find mode values using this method.

3.3 Modeling of a Single Link Flexible Manipulator

A description of the single-link manipulator system is considered, as shown in Fig. 3.1. *XOY* and *POQ* represent the stationary and moving coordinates respectively. Both axes lie in a horizontal plane and all rotation occurs about a vertical axis. $\tau(t)$ represents the applied torque at the hub by a drive motor, *E, I,* ρ and *A* represent the Young modulus, second moment of area, mass density per unit volume and cross-sectional area of the manipulator respectively. Transverse shear and rotary inertia effects are neglected in the link.

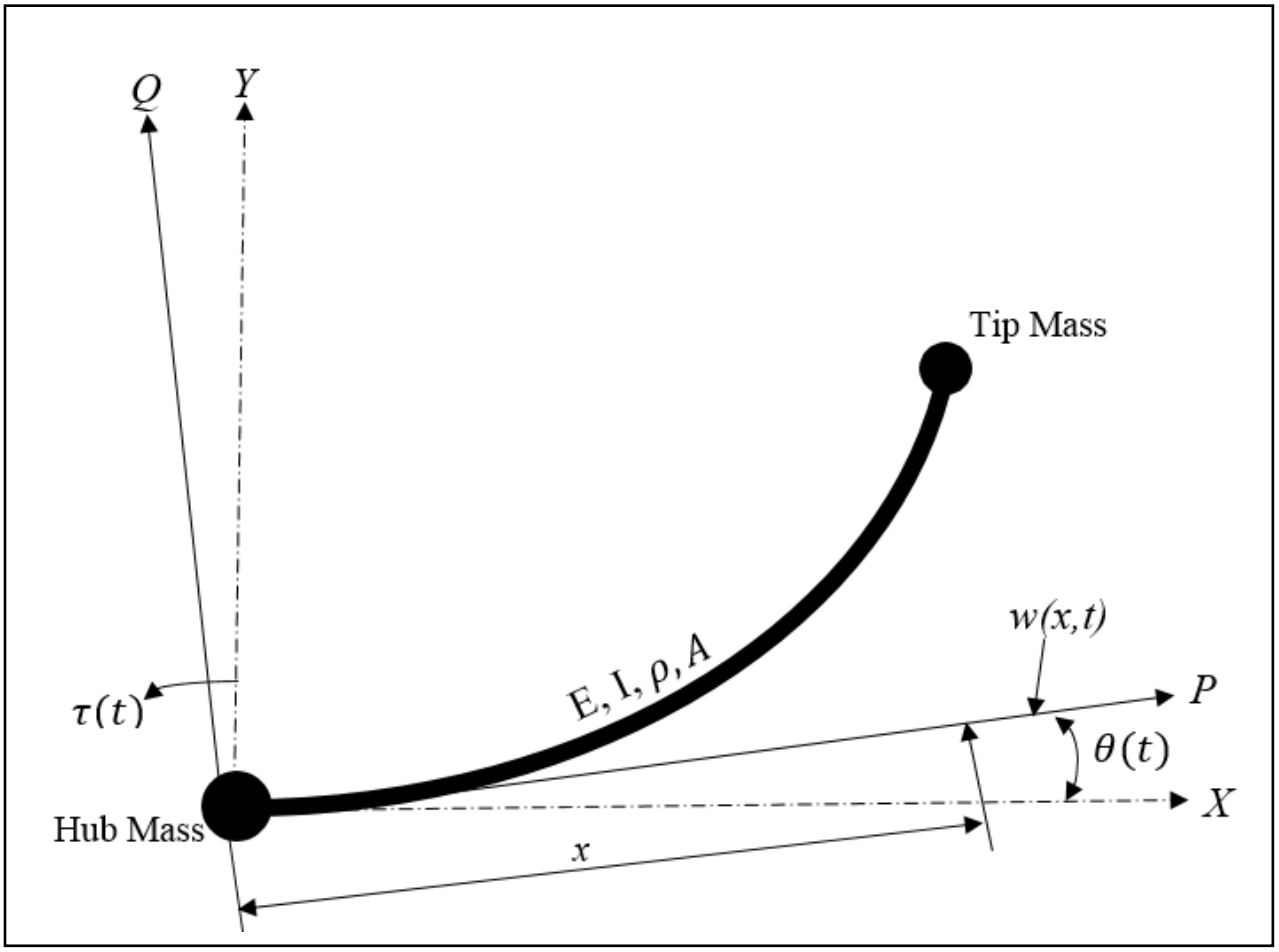

Fig. 3.1: Schematic diagram of a single-link flexible manipulator [12].

For angular displacement $\theta(t)$, elastic deflection $w(x,t)$ and total displacement $y(x,t)$ of a point along link at distance x from hub can be described as function of angular displacement and elastic deflection as

$$y(x,t) = x\theta(t) + w(x,t) \tag{3.1}$$

The velocity $v(x,t)$ of any point can be obtained as

$$v(x,t) = \frac{\partial y(x,t)}{\partial t} = x\frac{\partial \theta(t)}{\partial t} + \frac{\partial w(x,t)}{\partial t} \tag{3.2}$$

Using finite element method to solve dynamic problem leads to the equation,

$$w(x,t) = \boldsymbol{n}_l(x)\boldsymbol{q}_l(x) \tag{3.3}$$

where $\boldsymbol{n}_l(x)$ represent shape functions and $\boldsymbol{q}_l(t)$ represent nodal displacements.

The FEM requires two degrees-of-freedom at each node, one for transverse direction and other for rotation. These necessitate the use of Hermite cubic basic functions as element shape function

$$\boldsymbol{n_l}(x) = \begin{bmatrix} \phi_1(x) & \phi_2(x) & \phi_3(x) & \phi_4(x) \end{bmatrix} \tag{3.4}$$

where

$$\phi_1(x) = 1 - \frac{3x^2}{l^2} + \frac{2x^3}{l^3} \tag{3.5}$$

$$\phi_2(x) = x - \frac{2x^2}{l} + \frac{x^3}{l^2} \tag{3.6}$$

$$\phi_3(x) = \frac{3x^2}{l^2} - \frac{2x^3}{l^3} \tag{3.7}$$

$$\phi_4(x) = \frac{x^3}{l^2} - \frac{x^2}{l} \tag{3.8}$$

For each node, displacement vector [12] is given as,

$$\boldsymbol{q_l}(t) = [w_{n-1}(t) \quad \theta_{n-1}(t) \quad w_n(t) \quad \theta_n(t)]^T \tag{3.9}$$

where $w_{n-1}(t)$ and $w_n(t)$ are elastic deflections of element and $\theta_{n-1}(t)$ and $\theta_n(t)$ are corresponding angular displacements.

From Eqns. (3.1) and (3.3), the total displacement $y(x,t)$ can be written as,

$$y(x,y) = \boldsymbol{n_a}(x)\boldsymbol{q_a}(t) \tag{3.10}$$

where $\boldsymbol{n_a}(x) = [x \quad \boldsymbol{n_l}(x)]$ and $\boldsymbol{q_a}(t) = [\theta(t) \quad \boldsymbol{q_l}(t)^T]^T$ are the appended vectors in which the distance x and angle $\theta(t)$ denote global variables, $\boldsymbol{n_l}(t)$ and $\boldsymbol{q_l}(t)$ denote the local variables.

Among these, a local variable of n^{th} element is defined as

$$s = x - \sum_{i=1}^{n-1} l_i \tag{3.11}$$

where l_i is the length of n^{th} element.

Thus, the kinetic energy of n^{th} element can be expressed as

$$K.E._n = \int_o^l \rho A \left[\frac{\partial y(s,t)}{\partial t} \right]^2 ds$$

$$= \frac{1}{2} \int_o^l \rho A \left[y'^T y' \right] ds$$

$$= \frac{1}{2} \boldsymbol{q_a}^T \int_o^l \rho A \left[\boldsymbol{n_a}^T \boldsymbol{n_a} \right] \boldsymbol{q'_a} \tag{3.12}$$

The general representation of the kinetic energy is given as

$$K.E. = \frac{1}{2} \dot{\boldsymbol{q}}^T \boldsymbol{M} \dot{\boldsymbol{q}} \tag{3.13}$$

Compare Eqns. (3.12) and (3.13), the element mass matrix is found as

$$\boldsymbol{M}_n = \int_o^l \rho A \left[\boldsymbol{n_a}^T \boldsymbol{n_a} \right] ds \tag{3.14}$$

$$= \rho A \int_o^l \begin{pmatrix} 1 - \frac{3x^2}{l^2} + \frac{2x^3}{l^3} \\ x - \frac{2x^2}{l} + \frac{x^3}{l^2} \\ \frac{3x^2}{l^2} - \frac{2x^3}{l^3} \\ \frac{x^3}{l^2} - \frac{x^2}{l} \end{pmatrix} \begin{pmatrix} 1 - \frac{3x^2}{l^2} + \frac{2x^2}{l^3} \\ x - \frac{2x^2}{l} + \frac{x^3}{l^2} \\ \frac{3x^2}{l^2} - \frac{2x^3}{l^3} \\ \frac{x^3}{l^2} - \frac{x^2}{l} \end{pmatrix}^T dx \tag{3.15}$$

To demonstrate the process, one of the element of the mass matrix is calculated as follow

$$m_{22} = \rho A \int_0^l \left[1 - 3\left(\frac{x}{l} \right)^2 + 2\left(\frac{x}{l} \right)^3 \right]^2 dx$$

$$= \frac{13}{35} \rho A l = \frac{\rho A l}{420} \times 156 (3.16) \tag{3.16}$$

Following the similar procedure, all elements can be found to form the elemental mass matrix as

$$\boldsymbol{M}_n = \frac{\rho A l}{420} \left[\begin{array}{c|cccc} m_{11} & m_{12} & m_{13} & m_{14} & m_{15} \\ \hline m_{21} & 156 & 22l & 54 & -13l \\ m_{31} & 22l & 4l^2 & 13l & -3l^2 \\ m_{41} & 54 & 13l & 156 & -22l \\ m_{51} & -13l & -3l^2 & -22l & 4l^2 \end{array} \right] \tag{3.17}$$

where

$$\left.\begin{aligned} m_{11} &= 140l^2\left(3n^2-3n+1\right) \\ m_{12} &= m_{21} = 21l\left(10n-7\right) \\ m_{13} &= m_{31} = 7l^2\left(5n-3\right) \\ m_{14} &= m_{41} = 21l\left(10n-3\right) \\ m_{15} &= m_{51} = -7l^2\left(5n-2\right) \end{aligned}\right\} \tag{3.18}$$

The potential energy of the n^{th} element can be expressed as

$$\begin{aligned} P.E._n &= \frac{1}{2}\int_o^l EI\left[\frac{\partial^2 y(s,t)}{\partial s^2}\right]^2 ds \\ &= \frac{1}{2}\int_o^l EI\left[\left(B\boldsymbol{q_a}\right)^T B\boldsymbol{q_a}\right] ds \\ &= \frac{1}{2}\boldsymbol{q_a}^T\left[\int_o^l EI\left[B^T B\right] ds\right]\boldsymbol{q_a} \end{aligned} \tag{3.19}$$

where $B = \dfrac{d^2\boldsymbol{n_a}}{ds^2}$

The general representation of the potential energy is given as

$$P.E. = \frac{1}{2}\boldsymbol{q}^T\boldsymbol{K}\boldsymbol{q} \tag{3.20}$$

Compare Eqns. (3.18) and (3.19), the elemental stiffness matrix is found as

$$\begin{aligned} \boldsymbol{K}_n &= \int_o^l EI\left[B^T B\right] ds \\ &= EI\int_0^l \left[\frac{d^2\boldsymbol{n_a}}{ds^2}\right]^T\left[\frac{d^2\boldsymbol{n_a}}{ds^2}\right] ds \\ &= EI\int_0^l \frac{d^2}{dx^2}\left[\begin{pmatrix} 1-\dfrac{3x^2}{l^2}+\dfrac{2x^3}{l^3} \\ x-\dfrac{2x^2}{l}+\dfrac{x^3}{l^2} \\ \dfrac{3x^2}{l^2}-\dfrac{2x^3}{l^3} \\ \dfrac{x^3}{l^2}-\dfrac{x^2}{l} \end{pmatrix}^T\begin{pmatrix} 1-\dfrac{3x^2}{l^2}+\dfrac{2x^3}{l^3} \\ x-\dfrac{2x^2}{l}+\dfrac{x^3}{l^2} \\ \dfrac{3x^2}{l^2}-\dfrac{2x^3}{l^3} \\ \dfrac{x^3}{l^2}-\dfrac{x^2}{l} \end{pmatrix}\right] dx \end{aligned} \tag{3.21}$$

Solve for the first element of the stiffness matrix as

$$k_{11} = \frac{4EI}{l^4}\int_0^l \left(-3+6\frac{x}{l}\right)^2 dx \qquad (3.22)$$
$$= \frac{12EI}{l^3}$$

With the procedure, all the elements of the stiffness matrix can found and the final elemental stiffness matrix can be formed as

$$\boldsymbol{K}_n = \frac{EI}{l^3}\begin{bmatrix} 0 & 0 & 0 & 0 & 0 \\ 0 & 12 & 6 & -12l & 6l \\ 0 & 6l & 4l^2 & -6l & 2l^2 \\ 0 & -12 & -6l & 12 & -6l \\ 0 & 6l & 2l^2 & -6l & 4l^2 \end{bmatrix} \qquad (3.23)$$

3.3.1 Assembly of Elemental Matrices

Assemble the elemental mass and stiffness matrices by incorporating proper boundary conditions using the Lagrange equations of motion, the desired equations of motion of the system can be obtained as

$$\boldsymbol{M}\ddot{\boldsymbol{q}}(t) + \boldsymbol{D}\dot{\boldsymbol{q}}(t) + \boldsymbol{K}\boldsymbol{q}(t) = \boldsymbol{f}(t) \qquad (3.24)$$

where $\boldsymbol{M}$, $\boldsymbol{D}$ and $\boldsymbol{K}$ are global mass, damping and stiffness matrices of the manipulator respectively. $\boldsymbol{D}$ is a global damping matrix normally determined through experimentation. $\boldsymbol{f}(t)$ is a vector of external applied forces, of size $m \times 1$, where $m = 2n+1$. $\boldsymbol{q}(t)$ is a nodal displacement vector given as

$$\boldsymbol{q}(t) = \begin{bmatrix} \theta & w_o & \theta_0 & \ldots & w_n & \theta_n \end{bmatrix}^T \qquad (3.25)$$

where $w_n(t)$ and $\theta_n(t)$ are flexural and angular deflections at the end points of the manipulator respectively.

The global mass matrix can be represented as

$$\boldsymbol{M} = \sum_{e=1}^{n} M_e \qquad (3.26)$$

and can be represented into four sub matrices as

$$\boldsymbol{M} = \begin{bmatrix} \boldsymbol{M}_{\theta\theta} & \boldsymbol{M}_{\theta w} \\ \boldsymbol{M}_{\theta w} & \boldsymbol{M}_{ww} \end{bmatrix} \tag{3.27}$$

where, $\boldsymbol{M}_{ww}$ is elastic degree-of-freedom, $\boldsymbol{M}_{\theta w}$ represents coupling between elastic degree-of-freedom and $\boldsymbol{M}_{\theta\theta}$ is inertia of the system about hub axis.

The global stiffness matrix can be written as

$$\boldsymbol{K} = \sum_{e=1}^{n} K_e \tag{3.28}$$

and can be represented into four sub matrices as

$$\boldsymbol{K} = \begin{bmatrix} \boldsymbol{0} & \boldsymbol{0} \\ \boldsymbol{0} & \boldsymbol{K}_{ww} \end{bmatrix} \tag{3.29}$$

where, $\boldsymbol{K}_{ww}$ is the elastic degree of freedom. The stiffness matrix does not couple with the hub angle.

The $\boldsymbol{M}$ and $\boldsymbol{K}$ matrices are of size $m \times m$, where $m = 2n+1$. For the manipulator, considered as a pinned-free arm, with the applied torque at the hub, the flexural and rotational displacement, velocity and acceleration are all zero at the hub at $t = 0$ and the external force is $\boldsymbol{f}(t) = [\tau \quad 0 \ \ldots \ 0]^T$ and assume $q(0) = 0$.

From the elemental mass and stiffness matrices, the global mass and stiffness matrices can be generated, which are of the $size = 2n+3$.

For two elements, the extended mass matrix for first element can be written as

$$[\boldsymbol{M}]^1 = \frac{\rho A l}{420} \begin{bmatrix} m_{11} & m_{12} & m_{13} & m_{14} & m_{15} & 0 & 0 \\ m_{21} & 156 & 22l & 54 & -13l & 0 & 0 \\ m_{31} & 22l & 4l^2 & 13l & -3l^2 & 0 & 0 \\ m_{41} & 54 & 13l & 156 & -22l & 0 & 0 \\ m_{51} & -13l & -3l^2 & -22l & 4l^2 & 0 & 0 \\ 0 & 0 & 0 & 0 & 0 & 0 & 0 \\ 0 & 0 & 0 & 0 & 0 & 0 & 0 \end{bmatrix} \tag{3.30}$$

Substitute Eqn. (3.18) into (3.30) for $n = 1$

$$[\boldsymbol{M}]^1 = \frac{\rho Al}{420}\begin{bmatrix} 140l^2 & 63l & 14l^2 & 147l & -21l^2 & 0 & 0 \\ 63l & 156 & 22l & 54 & -13l & 0 & 0 \\ 14l^2 & 22l & 4l^2 & 13l & -3l^2 & 0 & 0 \\ 147l & 54 & 13l & 156 & -22l & 0 & 0 \\ -21l^2 & -13l & -3l^2 & -22l & 4l^2 & 0 & 0 \\ 0 & 0 & 0 & 0 & 0 & 0 & 0 \\ 0 & 0 & 0 & 0 & 0 & 0 & 0 \end{bmatrix} \tag{3.31}$$

For two elements, the extended mass matrix for second element can be written as

$$[\boldsymbol{M}]^2 = \frac{\rho Al}{420}\begin{bmatrix} m_{11} & 0 & 0 & m_{12} & m_{13} & m_{14} & m_{15} \\ 0 & 0 & 0 & 0 & 0 & 0 & 0 \\ 0 & 0 & 0 & 0 & 0 & 0 & 0 \\ m_{12} & 0 & 0 & 156 & 22l & 54 & -13l \\ m_{31} & 0 & 0 & 22l & 4l^2 & 13l & -3l^2 \\ m_{41} & 0 & 0 & 54 & 13l & 156 & -22l \\ m_{51} & 0 & 0 & -13l & -3l^2 & -22l & 4l^2 \end{bmatrix} \tag{3.32}$$

Substitute Eqn. (3.18) into (3.32) for $n = 2$

$$[\boldsymbol{M}]^2 = \frac{\rho Al}{420}\begin{bmatrix} 980l^2 & 0 & 0 & 273l & 49l^2 & 357l & -56l^2 \\ 0 & 0 & 0 & 0 & 0 & 0 & 0 \\ 0 & 0 & 0 & 0 & 0 & 0 & 0 \\ 273l & 0 & 0 & 156 & 22l & 54 & -13l \\ 49l^2 & 0 & 0 & 22l & 4l^2 & 13l & -3l^2 \\ 357l & 0 & 0 & 54 & 13l & 156 & -22l \\ -56l^2 & 0 & 0 & -13l & -3l^2 & -22l & 4l^2 \end{bmatrix} \tag{3.33}$$

Thus, global mass matrix can be obtained by adding extended matrices for first and second matrices as,

$$[\boldsymbol{M}]=\frac{\rho Al}{420}\begin{bmatrix} 1120l^2 & 63l & 14l^2 & 420l & 28l^2 & 357l & -56l^2 \\ 63l & 156 & 22l & 54 & -13l & 0 & 0 \\ 14l^2 & 22l & 4l^2 & 13l & -3l^2 & 0 & 0 \\ 420l & 54 & 13l & 312 & 0 & 54 & -13l \\ 28l^2 & -13l & -3l^2 & 0 & 8l^2 & 13l & -3l^2 \\ 357l & 0 & 0 & 54 & 13l & 156 & -22l \\ -56l^2 & 0 & 0 & -13l^2 & -3l^2 & -22l & 4l^2 \end{bmatrix} \tag{3.34}$$

With the help of same procedure, the global stiffness matrix can be obtained as

$$[\boldsymbol{K}]=\begin{bmatrix} 0 & 0 & 0 & 0 & 0 & 0 & 0 \\ 0 & 12 & 6l & -12 & 6l & 0 & 0 \\ 0 & 6l & 4l^2 & -6l & 2l^2 & 0 & 0 \\ 0 & -12 & -6l & 24 & 0 & -12 & 6l \\ 0 & 6l & 2l^2 & 0 & 8l^2 & -6l & 2l^2 \\ 0 & 0 & 0 & -12 & -6l & 12 & -6l \\ 0 & 0 & 0 & 6l & 2l^2 & -6l & 4l^2 \end{bmatrix} \tag{3.35}$$

3.3.2 Apply Boundary Conditions

The single-link flexible manipulator is considered as a pinned free beam, which imposes no rotational and transverse displacement on the first node. Thus, incorporating these boundary conditions on θ_1 and w_1 by eliminating respective rows and columns, the final representation of the mass matrix is written as

$$[\boldsymbol{M}]=\frac{\rho Al}{420}\begin{bmatrix} 1120l^2 & 63l & 14l^2 & 420l & 28l^2 & 357l & -56l^2 \\ 63l & 156 & 22l & 54 & -13l & 0 & 0 \\ 14l^2 & 22l & 4l^2 & 13l & -3l^2 & 0 & 0 \\ 420l & 54 & 13l & 312 & 0 & 54 & -13l \\ 28l^2 & -13l & -3l^2 & 0 & 8l^2 & 13l & -3l^2 \\ 357l & 0 & 0 & 54 & 13l & 156 & -22l \\ -56l^2 & 0 & 0 & -13l^2 & -3l^2 & -22l & 4l^2 \end{bmatrix} \tag{3.36}$$

$$\Rightarrow \qquad [\boldsymbol{M}] = \frac{\rho Al}{420}\begin{bmatrix} 1120l^2 & 420l & 28l^2 & 357l & -56l^2 \\ 420l & 312 & 0 & 54 & -13l \\ 28l^2 & 0 & 8l^2 & 13l & -3l^2 \\ 357l & 54 & 13l & 156 & -22l \\ -56l^2 & -13l^2 & -3l^2 & -22l & 4l^2 \end{bmatrix} \tag{3.37}$$

On the similar terms, the global stiffness matrix can be represented as

$$[\boldsymbol{K}] = \begin{bmatrix} 0 & 0 & 0 & 0 & 0 & 0 & 0 \\ 0 & 12 & 6l & -12 & 6l & 0 & 0 \\ 0 & 6l & 4l^2 & -6l & 2l^2 & 0 & 0 \\ 0 & -12 & -6l & 24 & 0 & -12 & 6l \\ 0 & 6l & 2l^2 & 0 & 8l^2 & -6l & 2l^2 \\ 0 & 0 & 0 & -12 & -6l & 12 & -6l \\ 0 & 0 & 0 & 6l & 2l^2 & -6l & 4l^2 \end{bmatrix} \tag{3.38}$$

$$\Rightarrow \qquad [\boldsymbol{K}] = \begin{bmatrix} 0 & 0 & 0 & 0 & 0 \\ 0 & 24 & 0 & -12 & 6l \\ 0 & 0 & 8l^2 & -6l & 2l^2 \\ 0 & -12 & -6l & 12 & -6l \\ 0 & 6l & 2l^2 & -6l & 4l^2 \end{bmatrix} \tag{3.39}$$

Adopting the same procedure, the mass and stiffness for any number of elements can be obtained.

3.3.3 State-Space Representation

The behavior of a system at any given time for any set of quantities is called state of the system. The quantities which determine the state are called state variables and the hypothetical space spanned by these state variables is called the state-space. The state variables are mathematically equated together within the state-space is called the state-space representation.

The matrix differential equation can be represented in a **state-space form** as

$$\begin{aligned} \dot{\boldsymbol{v}} &= \boldsymbol{Av} + \boldsymbol{Bu} \\ \boldsymbol{y} &= \boldsymbol{Cv} + \boldsymbol{Du} \end{aligned} \tag{3.40}$$

where $\boldsymbol{v} = [\theta \; w_1 \; \theta_1 \; \ldots \; w_n \; \theta_n \; \dot{\theta} \; \dot{w}_1 \; \dot{\theta}_1 \; \ldots \; \dot{w}_n \; \dot{\theta}_n]^T$ is called as the state-vector, $\boldsymbol{u} = \begin{bmatrix} \tau & 0 \ldots 0 \end{bmatrix}^T$ is known as the input vector and $\boldsymbol{A}, \boldsymbol{B}, \boldsymbol{C}$ and $\boldsymbol{D}$ are called as state-weighing coefficient matrices, which are given as

$$\boldsymbol{A} = \begin{bmatrix} \mathbf{0}_m & \boldsymbol{I}_m \\ -\boldsymbol{M}^{-1}\boldsymbol{K} & -\boldsymbol{M}^{-1}\boldsymbol{D} \end{bmatrix} \tag{3.41}$$

$$\boldsymbol{B} = \begin{bmatrix} \mathbf{0}_{m\times 1} \\ \boldsymbol{M}^{-1} \end{bmatrix} \tag{3.42}$$

$$\boldsymbol{C} = \begin{bmatrix} \mathbf{0}_m & \boldsymbol{I}_m \end{bmatrix} \tag{3.43}$$

$$\boldsymbol{D} = \begin{bmatrix} \mathbf{0}_{2m\times 1} \end{bmatrix} \tag{3.44}$$

In above equations, $\mathbf{0}_m$ is an $m \times m$ null matrix, $\boldsymbol{I}_m$ is an $m \times m$ identity matrix, $\mathbf{0}_{m\times 1}$ is an $m \times 1$ null matrix. The solution of the space state representation gives the state-vector $\boldsymbol{v}$, that is, the angular, nodal flexural and rotational displacements and velocities.

3.3.4 Validation of the Dynamic Model in Frequency Domain

Once the mathematical model is obtained, it is very important to validate the mathematical model. The reason being that input shaping very much sensitive to the uncertainties in the mathematical model. The performance of the shaper depends highly on the accuracy of the mathematical model. So, it is important to validate the model in terms of natural frequencies and damping ratios of the system. To make comparison, the parameter of the single-link flexible manipulator are chosen as same, as used by Tokhi et al. [12], as shown in Table 3.1

Table 3.1: Physical Parameters of the Single-Link Flexible Manipulator [12].

Name	**Symbol**	**Value**	**Units**
Link length	l	0.9	m
Width	b	19.008×10^{3}	m
Link thickness	h	3.2004×10^{3}	m
Modulus of elasticity	E	71×10^{9}	N/m^2
Hub inertia	I_{hub}	5.1924×10^{-11}	m^4
Density of Material	ρ	2710	Kg/m^3

Incorporating the above parameter values in Eqn. (3.34) and implying the boundary conditions, the global mass matrix is given as

$$\boldsymbol{M} = \begin{bmatrix} \boldsymbol{M}_{\theta\theta} & \boldsymbol{M}_{\theta w} \\ \boldsymbol{M}_{\theta w} & \boldsymbol{M}_{ww} \end{bmatrix}$$

$$= \begin{bmatrix} 0.04 & 0.01 & 0.00 & 0.03 & 0.00 & 0.03 & -0.00 \\ 0.01 & 0.03 & 0.00 & 0.01 & -0.00 & 0 & 0 \\ 0.00 & 0.00 & 0.00 & 0.00 & -0.00 & 0 & 0 \\ 0.03 & 0.01 & 0.00 & 0.06 & 0 & 0.01 & -0.00 \\ 0.00 & -0.00 & -0.00 & 0 & 0.00 & 0.00 & -0.00 \\ 0.03 & 0 & 0 & 0.01 & 0.00 & 0.03 & -0.00 \\ -0.00 & 0 & 0 & -0.00 & -0.00 & -0.00 & 0.00 \end{bmatrix}$$

$$= \begin{bmatrix} 0.04 & 0.03 & 0.00 & 0.03 & -0.00 \\ 0.01 & 0.01 & -0.00 & 0 & 0 \\ 0.00 & 0.00 & -0.00 & 0 & 0 \\ 0.03 & 0.06 & 0 & 0.01 & -0.00 \\ 0.00 & 0 & 0.00 & 0.00 & -0.00 \\ 0.03 & 0.01 & 0.00 & 0.03 & -0.00 \\ -0.00 & -0.00 & -0.00 & -0.00 & 0.00 \end{bmatrix} \quad (3.45)$$

Also, the global stiffness matrix for two elements, after implying the boundary conditions is:

$$\boldsymbol{K} = \begin{bmatrix} 0 & 0 \\ 0 & \boldsymbol{K}_{ww} \end{bmatrix}$$

$$= \begin{bmatrix} 0 & 0 & 0 & 0 & 0 & 0 & 0 \\ 0 & 485.48 & 109.23 & -485.48 & 109.23 & 0 & 0 \\ 0 & 109.23 & 32.77 & -109.23 & 16.38 & 0 & 0 \\ 0 & -485.48 & -109.23 & 970.96 & 0 & -485.48 & 109.23 \\ 0 & 109.23 & 16.38 & 0 & 65.54 & -109.23 & 16.38 \\ 0 & 0 & 0 & -485.48 & -109.23 & 485.48 & -109.23 \\ 0 & 0 & 0 & 109.23 & 16.38 & -109.23 & 32.77 \end{bmatrix}$$

$$= \begin{bmatrix} 0 & 0 & 0 & 0 & 0 \\ 0 & 970.96 & 0 & -485.48 & 109.23 \\ 0 & 0 & 65.54 & -109.23 & 16.38 \\ 0 & -485.48 & -109.23 & 485.48 & -109.23 \\ 0 & 109.23 & 16.38 & -109.23 & 32.77 \end{bmatrix} \quad (3.46)$$

After the implication of boundary conditions, applying the frequency functions in MATLAB, the resonance frequencies are calculated using the MATLAB function 'damp'. These frequencies are then compared with the resonance frequencies published in literature to validate the developed model. The comparison and relationship between number of elements and resonance frequencies of the system calculated and published are shown in Table 3.2.

Table 3.2: Comparison of resonant frequencies.

No. of elements	Resonant Frequencies in *Hz* reported by **Tokhi et al.** [12]			Resonant Frequencies in *Hz*, using **my MATLAB program**		
	Mode 1	Mode 2	Mode 3	Mode 1	Mode 2	Mode 3
1	14.49	47.7	-	14.36	47.45	-
2	11.99	35.71	77.17	13.37	35.55	76.69
3	11.99	35.46	65.68	13.33	35.26	65.38
5	11.99	35.46	65.43	13.31	35.13	65.24
10	11.99	35.22	65.2	13.31	35.11	65.04

Since, it is known that there are infinite degree of freedom for a flexible link and same number of modes of vibration, but only first three are reported in Table 3.2, because these three modes dominate over the rest of modes of vibration. It is found that, up to two places of decimal the first mode converges to 13.31 Hz, second mode converges to 35.11 Hz up and third mode at 65.04 Hz.

The resonance frequencies reported above for Tokhi et al. [12] may be miss-printed because the same model is used by same author in another publication [18], where the resonance frequencies are reported as 13 Hz, 35 Hz and 65 Hz. This process validates the accuracy of the dynamic

model in frequency domain, which is helpful in developing the input shaper for vibration suppression of the same manipulator in Chapter 5.

3.3.5 Validation of the Dynamic Model in Time Domain

In this section, the dynamic model of the flexible validated in time domain. The bang-bang torque is used as input for the simulation. The bang-bang torque is first positive and then negative impulse of 0.3 *Nm* amplitude. The simulated response of the single-link flexible manipulator due to bang-bang input torque is shown in Fig. 3.2 in terms of end point displacement, end point residual, hub angle and hub velocity without considering the damping.

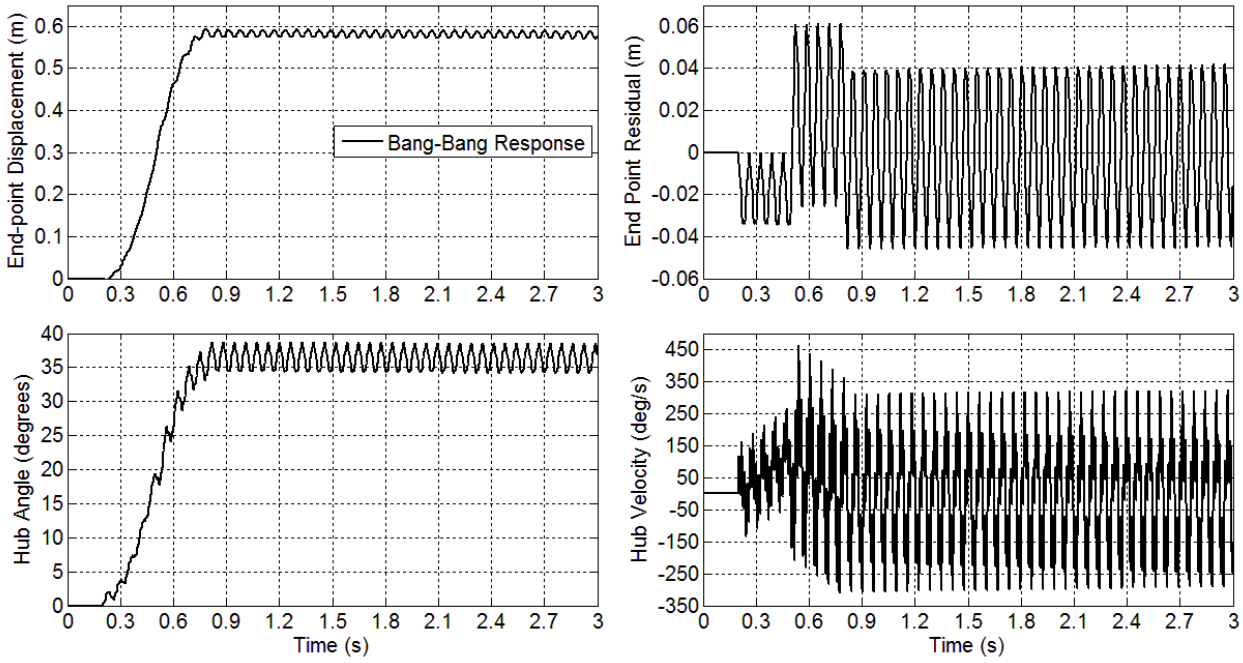

Fig. 3.2: Response of the single-link flexible manipulator for 1 element with no damping for end point displacement, end point residual, hub angle and hub velocity.

The level of the end point displacement is about 0.59 m and maximum hub angle is 38.7° approximately. This level of end point displacement is achieved in 0.78 *sec* and hub angle is reached in 0.81 *sec* using one element. The maximum end point residual is about 0.06136 m which is characterized by first mode of vibration and the maximum hub velocity is about 464 *deg/s.* As expected, the system show persistent oscillatory response, thus validating the dynamic

model accurate in the time domain. The response of the flexible system is found in close agreement with the one reported by Tokhi et al. [12].

3.4 Summary

The dynamic model has been developed using finite element method. Using MATLAB program, the resonant frequencies have been obtained and compared to the published literature. The accurate mathematical model developed in this Chapter, after completely validating it in both frequency and time domain, is helpful to obtain correct input shaper for vibration suppression of the flexible manipulators, which is being developed in the Chapter 4.

CHAPTER 4 CONTROL OF FLEXIBLE MANIPULATORS

4.1 Introduction

The control of flexible manipulators is to maintain accurate positioning is an extremely challenging problem. Due to the flexible nature and distributed characteristics of the system, the dynamics are highly nonlinear and complex. Problems arise due to precise positioning requirement, vibration due to system flexibility and the difficulty in obtaining accurate model of the system. Therefore, flexible manipulators have not been much favored in production industries, due to unattained endpoint positional accuracy requirements in response to input commands. A hybrid controller is very good in such cases which helps in reducing vibrations from the combination of command shaping and feedback control. In this respect, a control mechanism that accounts for both the rigid body and the flexural motions of the system is required.

The control strategies for flexible manipulators can be classified as **feedforward** (open loop) control and **feedback** (closed-loop) control.

Feedforward Control techniques for vibration suppression involves developing the control input through consideration of the physical and vibrational properties of the system, so that system vibrations at response modes are reduced. A block diagram of feedforward control [20] is shown in Fig. 4.1. This method does not require any additional sensors or actuators and does not account for changes in the system, once the input is developed.

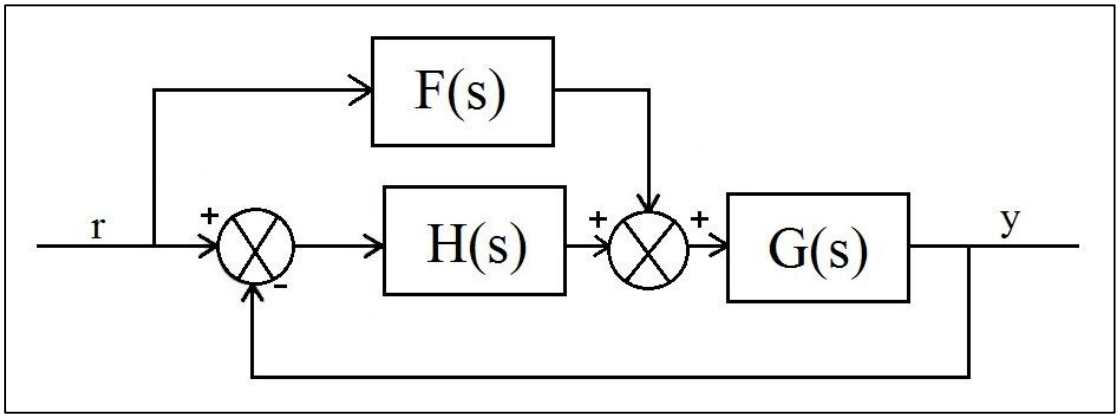

Fig. 4.1: Block diagram of feedforward control scheme

Feedback Control techniques uses measurement and estimations of the system states to reduce vibration. Feedback controllers are designed to be robust to parameter uncertainty. The complexity of the required feedback controllers can be reduced further. Fig. 4.2 shows a blocked diagram of feedback control [21].

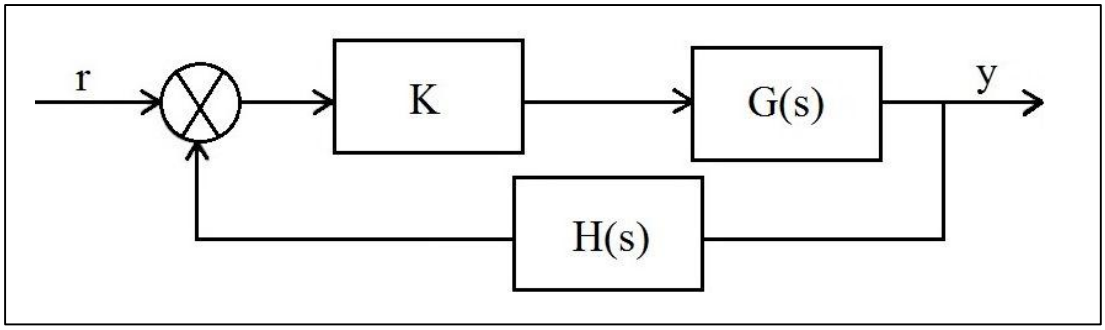

Fig. 4.2: Block diagram of feedback control scheme

4.2 Input shaping

A technique for vibration suppression of flexible manipulators is known as **command shaping technique**. In this technique, shaped torque input is developed on the basis of extracting input energy around the natural frequencies of the system, so that the vibration of the flexible manipulators while moving is reduced.

The design objectives in input shaping are to determine the amplitude and time locations of the impulses, so that shaped command reduces the detrimental effects of system flexibility. It involves the suppression of the vibration generated by an impulse to the vibration generated by another. The shaper parameters are amplitude and time instants of the impulse, which are functions of natural frequencies and damping ratios of the physical model i.e.

$$\text{Shaper} = \begin{bmatrix} A \\ t \end{bmatrix} = f(\omega, \zeta) \tag{4.1}$$

where ω denotes the natural frequency and ζ denotes the damping ratio.

4.2.1 Basis of Input Shaping

To understand the concept of input shaping, let's start with simplest command - an impulse. This method involves convolving desired commands with a sequence of impulses, in a way that vibration produced by first impulse is suppressed by another impulse. For example, an impulse signal of size A_1 in the response of underdamped system is induced to create the vibration in the system, as shown in Fig. 4.3.

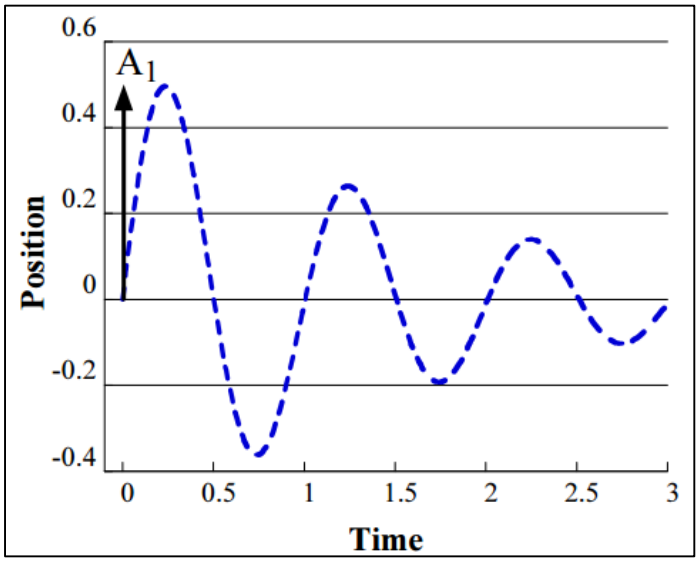

Fig. 4.3: First impulse response.

Another impulse of calculated magnitude A_2 at another time is induced to cancel the vibration induced by the first impulse, as shown in Fig. 4.4. The second impulse must be applied at the correct time and must have the appropriate magnitude for complete cancellation of impulse prior.

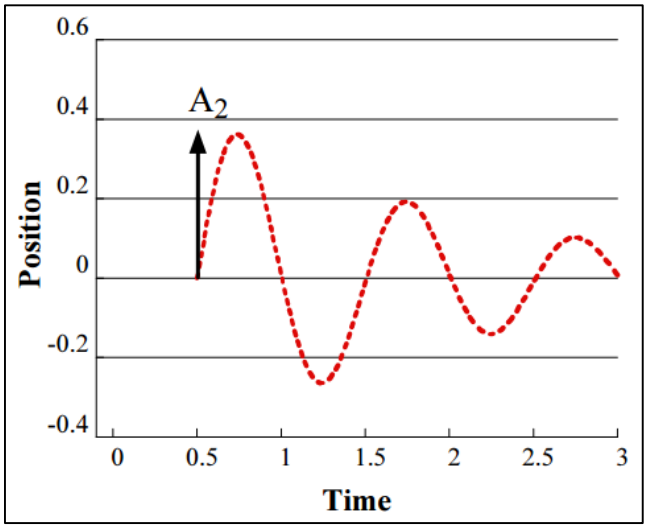

Fig. 4.4: Second impulse response.

Now, combining the two responses results in zero residual vibration. The resultant response of both the impulses A_1 and A_2 is shown in Fig. 4.5. This approach can be utilized computing impulses together to form a sequence of impulses that attenuate vibration at higher modes.

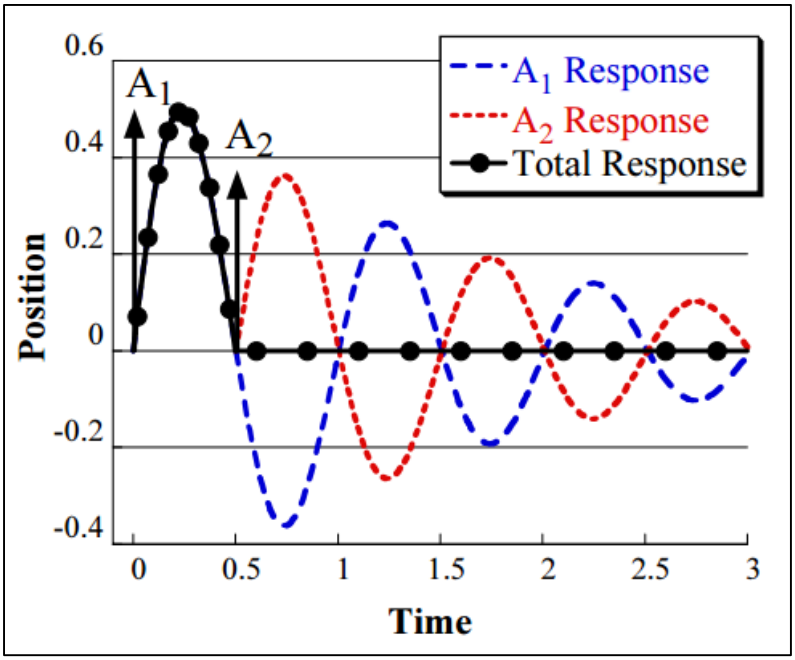

Fig. 4.5: Total response from overlapping of both impulses.

4.2.2 Development of an Input Shaper

Amplitude and time location of the impulses are the design objectives in an input shaper. The method is briefly explained. A vibratory system can be modeled as superposition of second order system each with transfer function as

$$G(s) = \frac{\omega^2}{s^2 + 2\zeta\omega s + \omega^2} \tag{4.2}$$

The impulse response of the system can be written as

$$y(t) = \frac{A\omega}{\sqrt{1-\zeta^2}} e^{-\zeta\omega(t-t_0)} \sin\left(\omega\sqrt{1-\zeta^2}(t-t_0)\right) \tag{4.3}$$

where A and t_0 are amplitude and time of the impulse respectively.

Further, the response to a sequence of impulses can be obtained by superposition of the impulses. Thus, for N nunber of impulses with damped frequency as $\omega_d = \omega\sqrt{1-\zeta^2}$, the impulse response [18] can be expressed as

$$y(t) = M\sin(\omega_d t + \alpha) \tag{4.4}$$

where

$$M = \sqrt{\left(\sum_{i=1}^{N} B_i \cos\phi_i\right)^2 + \left(\sum_{i=1}^{N} B_i \sin\phi_i\right)^2} \tag{4.5}$$

$$B_i = \frac{A_i\omega_n}{\sqrt{1-\zeta^2}} e^{-\omega\zeta(t-t_i)} \tag{4.6}$$

$$\phi_i = \omega_d t_i \tag{4.7}$$

A_i and t_i are the amplitude and time of the i^{th} impulse.

The residual single mode vibration amplitude of the impulse response, obtained at time of last impulse t_N, is given as

$$V = \sqrt{V_1^2 + V_2^2} \tag{4.8}$$

where

$$V_1 = \sum_{i=1}^{N} \frac{A_i\omega_n}{\sqrt{1-\zeta^2}} e^{-\zeta\omega_n(t_N - t_i)} \cos\left(\omega_d t_i\right) \tag{4.9}$$

$$V_2 = \sum_{i=1}^{N} \frac{A_i\omega_n}{\sqrt{1-\zeta^2}} e^{-\zeta\omega_n(t_N - t_i)} \sin\left(\omega_d t_i\right) \tag{4.10}$$

For zero vibration after last impulse, both V_1 and V_2 must be independently zero. If sum of amplitudes of impulses is unity, then shaped command input produces same rigid body motion as unshaped command. The first impulse is selected at $t_1 = 0$ for avoiding response delay. Setting V_1 and V_2 of the equations as zero,

$$\sum_{i=1}^{N} A_i = 1 \tag{4.11}$$

and on solving yields a two impulse sequence with parameters as

$$t_1 = 0 \qquad A_1 = \frac{1}{1+K} \tag{4.12}$$

$$t_2 = \frac{\pi}{\omega_d} \qquad A_2 = \frac{K}{1+K} \tag{4.13}$$

where

$$K = e^{-\frac{\zeta\pi}{\sqrt{1-\zeta^2}}} \tag{4.14}$$

Writing the above time and amplitudes in the form of matrix as

$$\begin{bmatrix} t_i \\ A_i \end{bmatrix} = \begin{bmatrix} 0 & \frac{\pi}{\omega_d} \\ \frac{1}{1+K} & \frac{K}{1+K} \end{bmatrix} \tag{4.15}$$

This is called as Zero Vibration (ZV) Shaper [19] because residual vibration is zero, when there is no error in the modeled frequency.

To handle higher vibration modes, an impulse sequence for each vibration mode can be designed independently. For any vibratory system, the vibration reduction can be accomplished by convolving any desired system input with impulse sequence. This yields a shaped input that drives the system to a desired location without vibration.

ZV shaper theoretically yield zero-vibration at the modeling frequency, still it is very sensitive to modeling errors. This sensitivity to modeling errors prohibited the ZV shaper from practical use on many systems. To reduce the sensitivity of the input shaper for errors in natural frequency, the derivative of the vibration with respect to the natural frequency is set to zero. Due to this constraint on residual vibration, it requires the addition of another impulse. This yields the following impulse times and amplitudes

$$\begin{bmatrix} t_i \\ A_i \end{bmatrix} = \begin{bmatrix} 0 & \frac{\pi}{\omega_d} & \frac{2\pi}{\omega_d} \\ \frac{1}{1+2K+K^2} & \frac{2K}{1+2K+K^2} & \frac{K^2}{1+2K+K^2} \end{bmatrix} \tag{4.16}$$

This developed shaper adds the robustness constraint of zero-derivative at the modeling frequency, so it is called the Zero-Vibration Derivative (ZVD) shaper [19]. This process of equating derivatives equal to zero can be further implemented with higher order derivatives. Each higher order derivative constraint requires the addition of another impulse. This increases the robustness of the shaper and increases the rise time of the system.

4.2.3 Robustness of the Shaper

Robustness is a desirable property that dictates, whether the system is immune to uncertainties in its mathematical model. To increase the system robustness, certain assumptions are included in the modeling. The shaper formed above is sensitive to modeling errors, because it is formed using constraints that limit the vibration of the system to zero only at exact natural frequency and damping ratio of the system. In real applications, these parameters required to form the input shaper are not known exactly. Therefore, a robust shaper is required which can compensate modeling errors in itself. To remove the system error or limit them, various robust input shapers are designed.

4.2.4 Applications of Input Shaping

Input shaping is very useful in vibration reduction in a number of mechanical systems. For example, mechanical systems like cranes, flexible space crafts etc. Both cranes and flexible spacecraft sometimes oscillate with long periods and have little to no damping. This means that any vibration induced in the system will continue for a long time unless controlled quickly. Thus, input shaping can be extremely useful in reducing induced vibrations and increasing the speed and accuracy of such systems. Singhose [19] has mentioned about implementation of input shaping on a gantry crane, coordinate measuring machine and MACE experiment in space.

4.3 Linear Feedback Controller

An important aspect of feedback system design is the stability of the control system. The main goal of a feedback design is to stabilize a system if it is not stable initially or improve the stability later. The stability of linear systems can be improved by state feedback.

4.3.1 Proportional-Derivative (PD) Control

The aim of using proportional-derivative controller is to increase the stability of the system by improving control since it has an ability to predict the future error of the system response. In order to avoid effects of the sudden change in the value of the error signal, the derivative is taken from the output response of the system variable instead of the error signal.

To demonstrate the performance of the vibration control schemes, a proportional-derivative feedback control of collocated sensor signals is adopted for control of rigid body motion of the manipulator. A block diagram of the PD controller [18] is shown in Fig. 4.6.

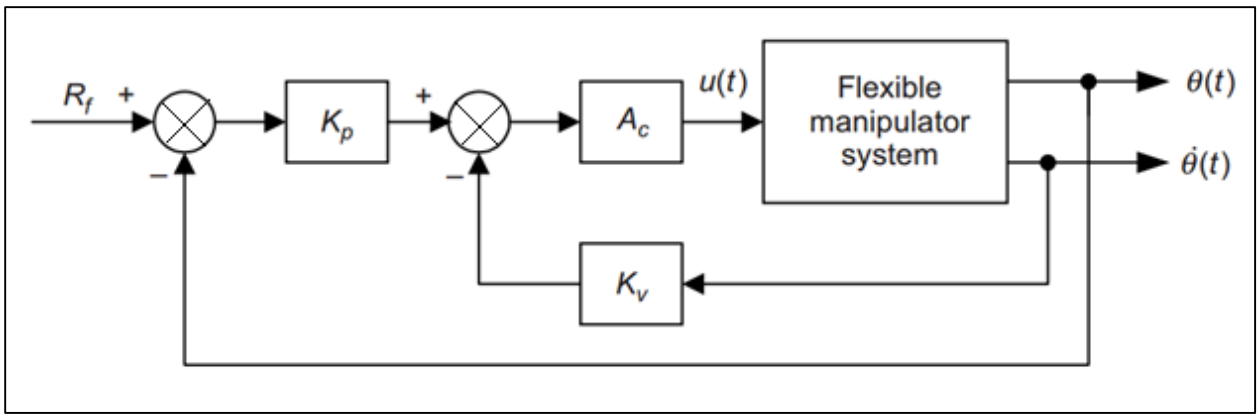

Fig. 4.6: The proportional derivative control structure [18].

K_P and K_V are the proportional and derivative gains respectively, θ represents hub angle, $\dot{\theta}$ represents hub velocity, R_f is the reference hub angle and A_c is the linear gain of the motor amplifier. Essentially, the task of this controller is to position the flexible arm to the specified angle as required. The hub angle and hub velocity signals are fed back and used to control the hub angle of the manipulator. The control signal $U(s)$ can thus be obtained as

$$U(s) = A_c\left[K_P\left\{R_f(s) - \theta(s)\right\} - K_V s\theta(s)\right] \tag{4.17}$$

Here, s is the Laplace variable. Hence the closed-loop transfer function is obtained as

$$\frac{\theta(s)}{R_f(s)} = \frac{K_P H(s) A_c}{1 + A_c K_V (s + (K_P/K_V))H(s)} \tag{4.18}$$

Here, $H(s)$ is the open loop transfer function from the input torque to the hub angle of the system provided as

$$H(s) = C(sI - A)^{-1}B \tag{4.19}$$

Thus, the closed-loop poles of the system are given by the characteristics equation as

$$1 + K_V (s + Z) H(s) A_c = 0 \tag{4.20}$$

Here, $Z = K_P / K_V$ represents the compensator zero which determines the control performance of the closed-loop system.

4.4 Hybrid Controller

In this work, a hybrid controller is developed which is based on the combination of command shaping and feedback control scheme. The hybrid controller provides much better stability to the system with the help of improved control over the vibrations of the flexible system. The modified block diagram for a hybrid controller is shown in Fig. 4.7.

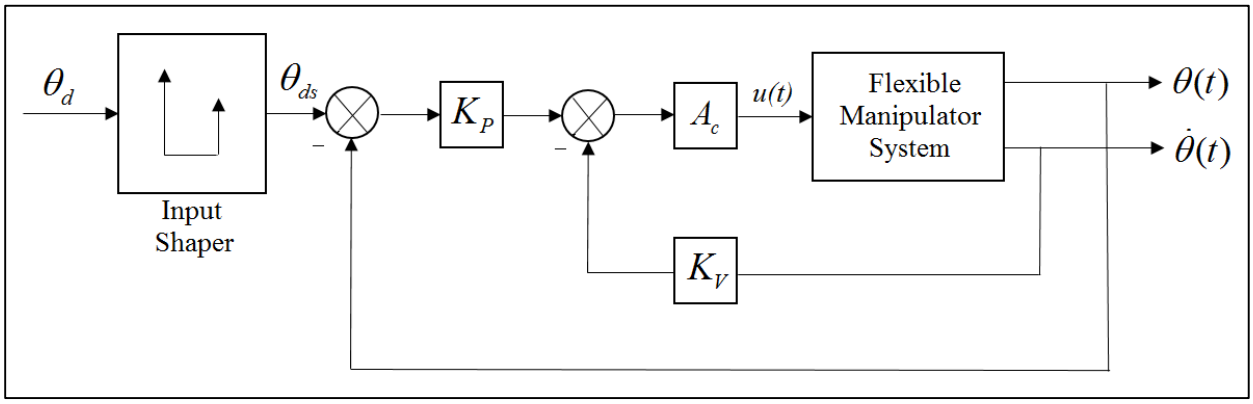

Fig. 4.7: Block diagram of a hybrid controller

In the Fig. 4.8, K_P and K_V are the proportional and derivative gains respectively and A_c is linear gain of the motor. θ_d is the reference hub angle and θ_{ds} is the shaped hub angle. The hub angle is controlled by the feedback response of the hub angle and hub velocity. The modified control signal $U(s)$ can thus be obtained as

$$U(s) = A_c \left[K_P \left\{ \theta_{ds}(s) - \theta(s) \right\} - K_V s\theta(s) \right] \tag{4.27}$$

where s is the Laplace variable. Hence the modified closed-loop transfer function is obtained as

$$\frac{\theta(s)}{\theta_{ds}(s)} = \frac{K_P H(s) A_c}{1 + A_c K_V (s + (K_P / K_V)) H(s)} \tag{4.28}$$

where $H(s)$ is the open loop transfer function from the input torque to the hub angle of the system provided as

$$H(s) = C(sI - A)^{-1} B \tag{4.29}$$

Thus, the characteristics equation for the closed loop of the poles can be written as

$$1 + K_V (s + Z) H(s) A_c = 0 \tag{4.30}$$

Here, $Z = K_P / K_V$ represents the compensator zero responsible for the control performance of the closed-loop system.

4.5 Summary

In this Chapter, the control of the flexible manipulator has been discussed. The concept of command shaping for vibration suppression of flexible manipulators has been presented. The basis of input shaping has been discussed in brief and an analytical formulation of the shaper has been presented. A linear state feedback control scheme has been utilized to achieve high positional accuracy. Also, a hybrid controller has been developed with the combination of command shaping and feedback control. The dynamic model has been implemented on this control scheme for the vibration suppression of the flexible manipulator and the results are presented in the Chapter 5.

CHAPTER 5 RESULTS AND DISCUSSIONS

5.1 Introduction

In this chapter, results are simulated for the dynamic model of the single-link flexible manipulator in time domain for different modes of frequencies. Various simulations are presented for three different modes to show the response of the flexible manipulator in open loop control and input shaping is implemented for suppression of vibration in the flexible manipulator. Later in the chapter, a proportional-derivative control scheme is used for vibration suppression of flexible manipulator in closed-loop control. The dynamic model was developed and implemented for control in MATLAB environment.

5.2 Vibration Suppression using Open-Loop Control

The vibrations produced in the flexible manipulator are required to be suppressed or minimized. In this section, an open-loop control with input shaping is implemented for vibration suppression. A bang-bang input torque of 0.3 *Nm* is applied to the dynamic model and results are shown in Fig. 5.1. The problem with unshaped bang-bang input torque is that the flexible manipulator cannot achieve torque of 0.3 *Nm* in minimum time.

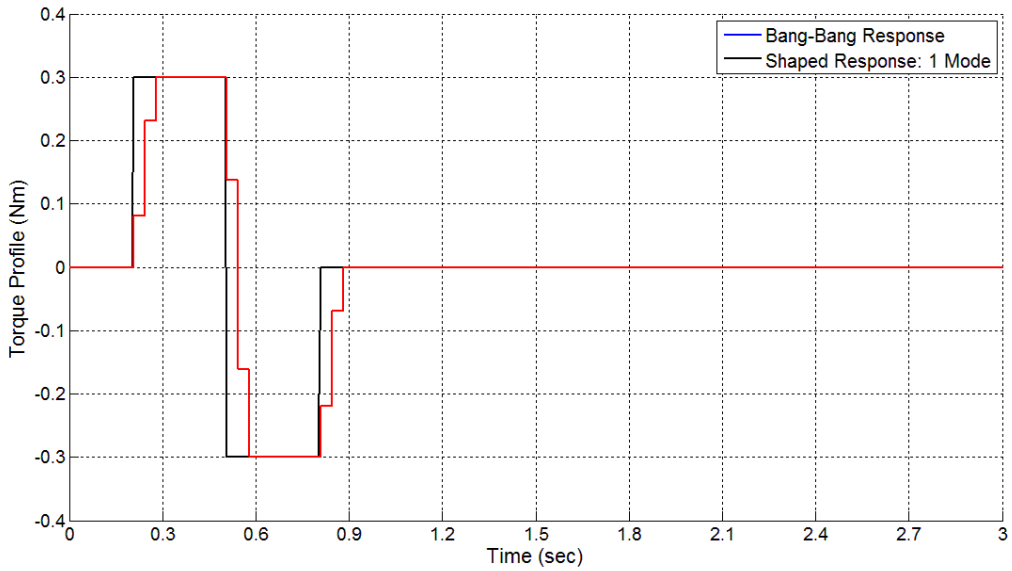

Fig. 5.1: Simulated response of single-link flexible manipulator for 3 number of elements for bang-bang vs. shaped response for 1 mode

Even if this is possible, the manipulator will vibrate at very high velocities and can cause great deflections while achieving a desired position. Thus, it is required to shape or pre-process the input torque profile so that the manipulator takes little time to achieve an amplitude with minimum vibrations and optimum speed.

Using the same physical parameters of the single-link flexible manipulator, as given in Table 3.1 and resonant frequencies, as given in Table 3.2, the ZVD shaper is found as

$$\begin{bmatrix} A \\ t \end{bmatrix} = \begin{bmatrix} 0.230 & 0.221 & 0.219 \\ 0.072 & 0.022 & 0.009 \end{bmatrix} \tag{5.1}$$

The input torque profile is required to be interpolated. Fig. 5.1 shows the response of shaped input response against the unshaped bang-bang input torque for only first mode of frequency for 3 impulses. The simulation is run for 3 seconds and 3 elements are considered to obtain the dynamic model. In this figure, it is clear that how input is shaped and the time for the manipulator to gain first positive amplitude of 0.3 *Nm* about 0.28 *sec*.

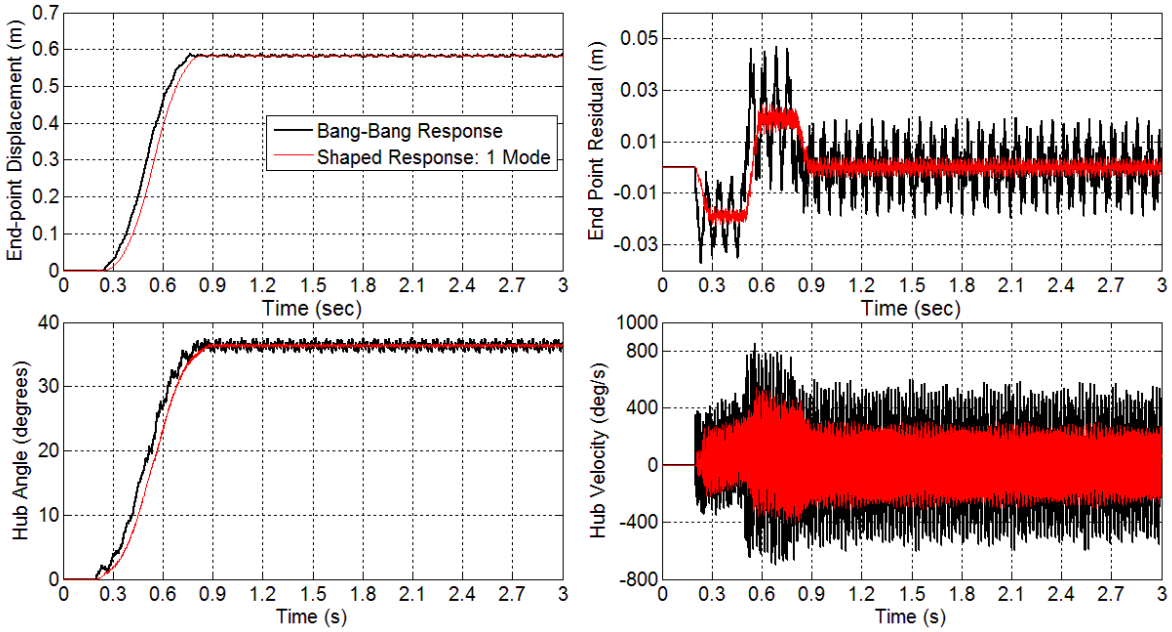

Fig. 5.2: Comparison of bang-bang vs 1-mode shaped response of the single-link flexible manipulator in terms of end point displacement, end point residual, hub angle and hub velocity.

Fig 5.2 shows the vibration levels for both unshaped and shaped torque inputs in terms of end point displacement, end point residual, hub angle and hub velocity for 3 elements. It can be noted that the desired trajectory is achieved in shaped response very smoothly. The hub angle of $36.66°$ is achieved within 0.88 *sec* and it vibrates in range of $36.17° - 36.66°$ for the rest of the time where as in unshaped case, the hub vibrates between $35.3° - 37.5°$. The maximum hub velocity is decreased from 849.5 *deg/s* to 547.7 *deg/s*, reduced by 35.52%. The end point displacement is achieved within time 0.2 *sec* less than unshaped input. The maximum level of the end point residual is reduced 47.8% by the shaped input torque just by using 1 mode of frequency of the system.

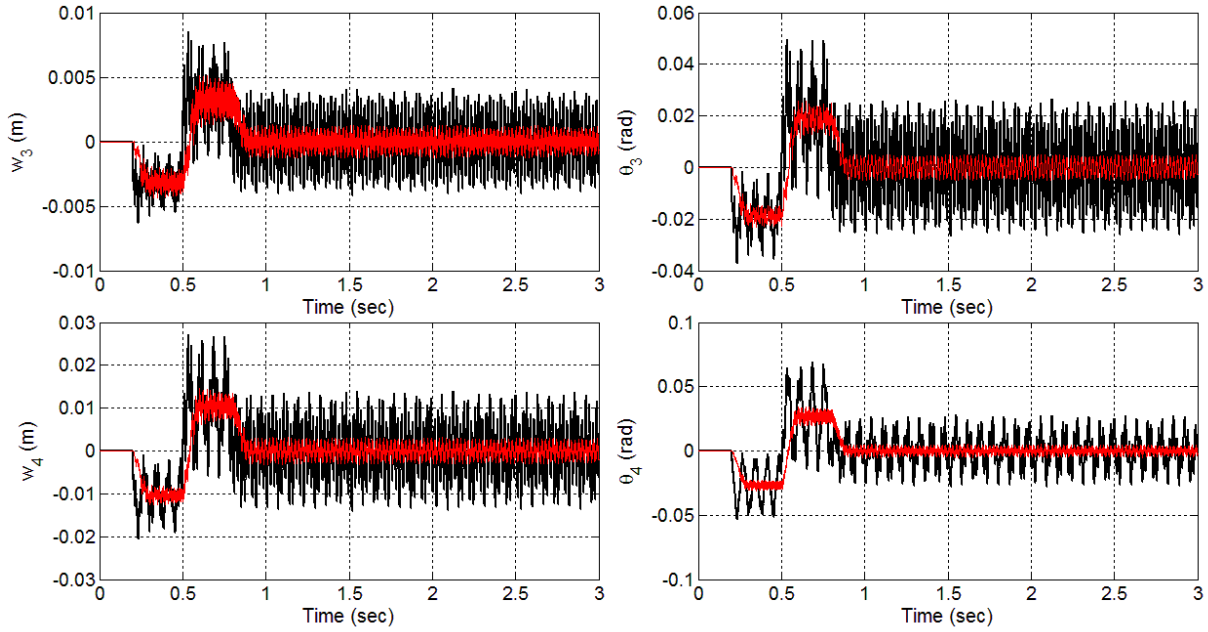

Fig. 5.3: Comparison of bang-bang vs 1-mode shaped response of the single-link flexible manipulator for 3 elements in terms of elastic deflections and angular displacements.

From the Fig. 5.3, it is clear that the elastic deflections and angular displacements are reduced greatly with the shaped response. In case of elastic deflection w_3, the maximum deflection has been decreased from 0.00849 *m* to 0.00513 *m*. The maximum reduction in angular position of the link of the manipulator is 0.24 *rad*. In case of elastic deflection w_4, the maximum deflection of the shaped response is 0.00144 *m* which was previously 0.0272 *m* in case of unshaped response. For the respective angular deflection θ_4, the maximum deflection is reduced by 0.0353 *rad*.

Now, the same simulation is run for two modes of vibrations for three seconds. The number of elements and impulses considered are three. The input torque profile for unshaped bang-bang response and shaped response of one mode as well as two modes is shown in Fig. 5.4. It can be noted that for 2 modes of vibration, the input torque profile has been interpolated very fine as compared to 1 mode shaped response and unshaped response. The amplitude of 0.3 *Nm* is achieved in 0.302 *sec.* The number of elements for 2 modes of vibrations are three and simulation is run for 3 seconds to check the response of input torque profiles.

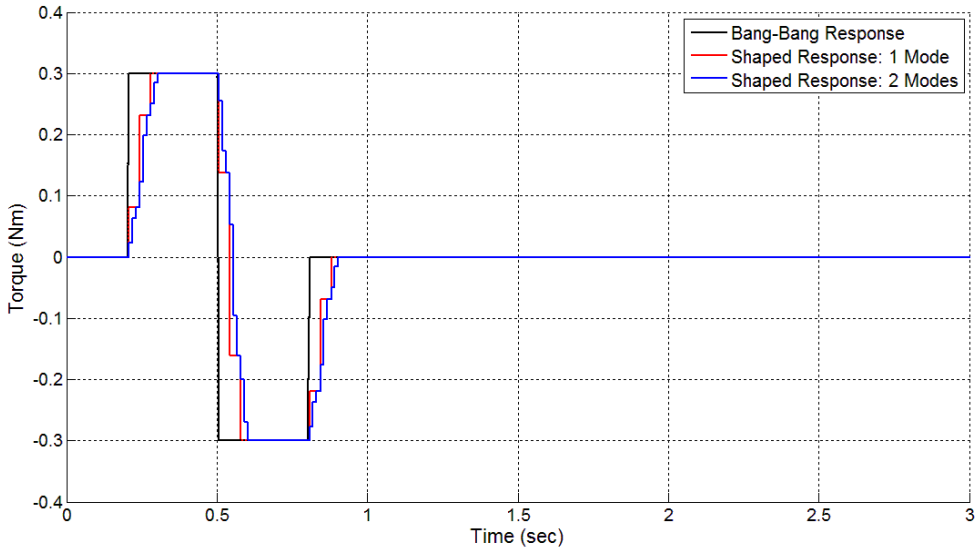

Fig. 5.4: Bang-bang response vs 1 mode shaped response vs 2 modes shaped response

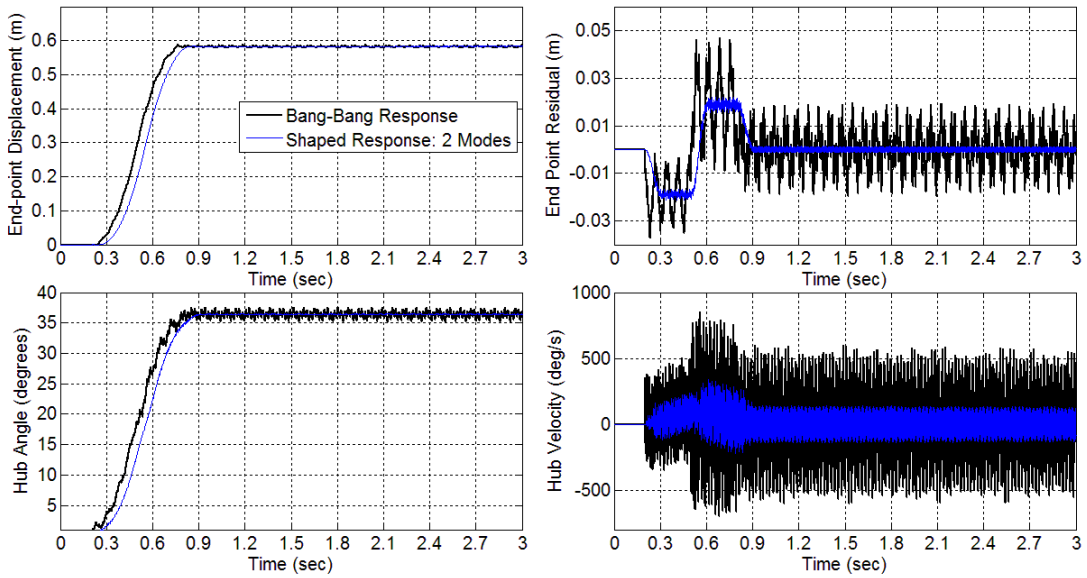

Fig. 5.5: Comparison of bang-bang vs 2-mode shaped response of the single-link flexible manipulator for 3 elements for end point displacement, end point residual, hub angle and hub velocity.

In Fig. 5.5, the response of the 2 modes shaped input is even better than 1 mode of frequency. The maximum hub angle in 2 modes shaped response is 36.47 *deg* and it vibrates in range of 36.31 *deg* to 36.57 *deg*. The maximum end point displacement of 0.58 *m* is achieved within 0.85 *sec* which is 0.05 *sec* and 0.1 *sec* less than 1 mode shaped response and unshaped response respectively. The maximum end point residual in 2 mode shaped response is reduced from 0.04705 *m* to 0.02211 *m*. The hub highest velocity is reduced by from 849.5 *deg/s* to 339.9 *deg/s* as seen in the above figure. In other words that can be said that the vibration levels are reduced by 59.98%.

Also, the elastic deflections and angular displacements are affected with the change in modes of vibrations from one to two modes. Fig. 5.6 shows the comparison of response of single-link flexible manipulator in terms of elastic deflections and angular displacements of the elements for 2 modes. With 2 modes, the elastic deflections and angular displacements are reduced better with the shaped signal. In case of elastic deflection w_3, the maximum deflection has been reduced from 0.008497 *m* to 0.004347 *m*. The respective maximum angular position of the link element is 0.022 *rad*. In case of elastic deflection w_4, the maximum deflection of the shaped response reduced from 0.0272 *m* to 0.0124 *m*. For the respective angular deflection θ_4, the maximum deflection is 0.031 *rad* for shaped response.

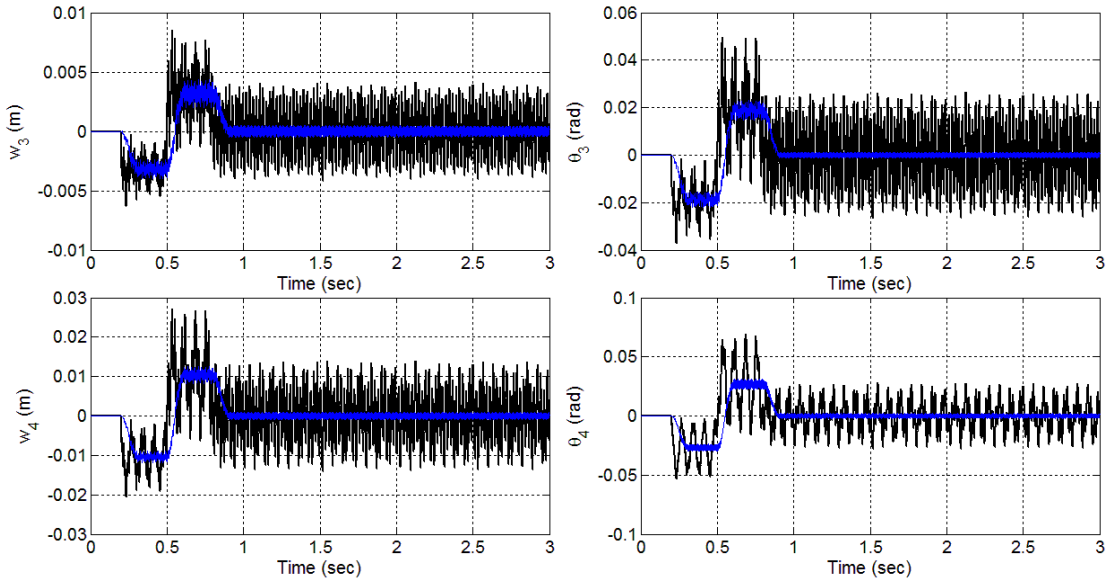

Fig. 5.6: Comparison of bang-bang vs 2-mode shaped response of the single-link flexible manipulator for 3 elements in terms of elastic deflections and angular displacements.

All the aspects of the manipulator are affected greatly with the shaping of input torque. Now, for 3 modes of vibrations, all the aspects of the flexible manipulator should be more precise towards their levels of vibration. The input torque profile for three modes of vibrations is shown in Fig. 5.7 along with the input bang-bang torque profile. With the increase in number of modes, the plot for shaped input profile becomes smoother than precious profiles. The first positive impulse of 0.3 *Nm* is achieved by 3 modes of vibrations in 0.312 *sec*.

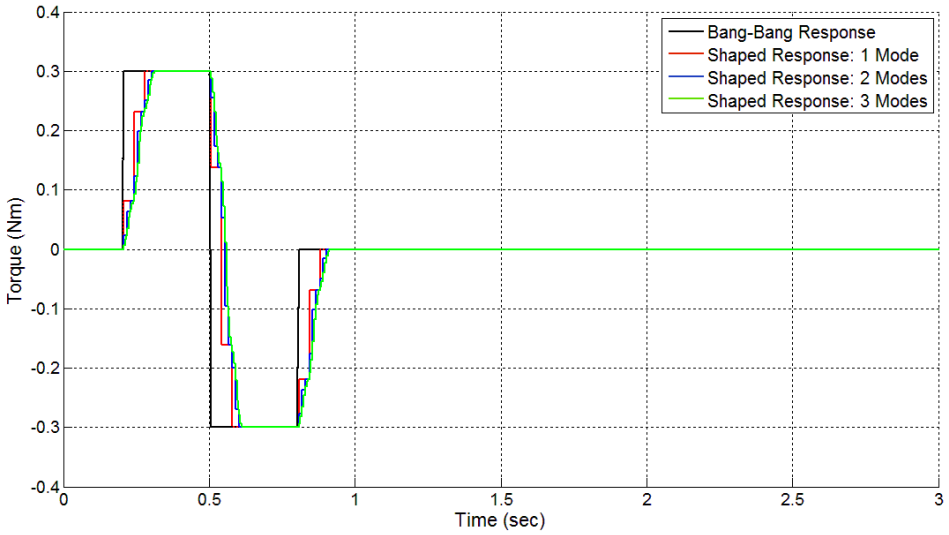

Fig. 5.7: Bang-bang response vs 1 mode vs 2 modes vs 3 modes shaped response

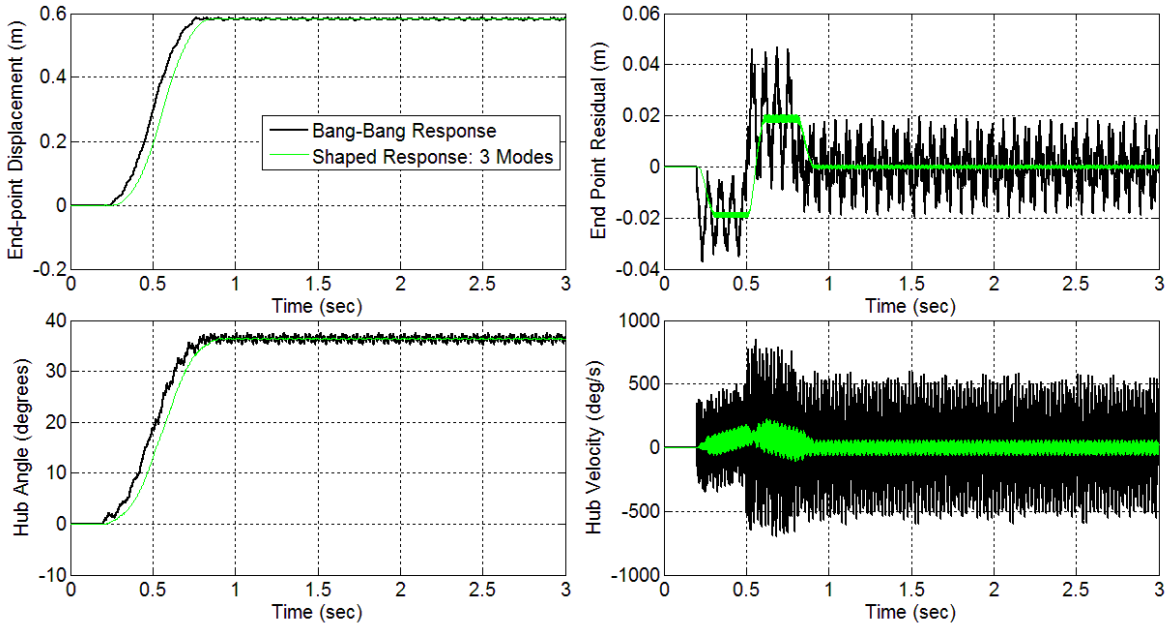

Fig. 5.8: Comparison of bang-bang vs 3-mode shaped response of the single-link flexible manipulator for 3 number of elements for end point displacement, end point residual, hub angle and hub velocity.

In Fig 5.8, the shaped response for 3 modes of vibrations is shown. The maximum hub angle in shaped response of 3 modes is 36.42 *deg*, a little less than 2 shaped response and it vibrated in the range of 36.34 *deg* to 36.42 *deg*. The maximum end point displacement of 0.583 *m* is achived within 0.84 *sec*. The maximum end point residual in 2 mode shaped input is reduced by 0.0266 *m*. The maximum hub velocity is reduced from 849.5 *deg/s* to 231.7 *deg/s* as seen in the above figure. The hub velocity is reduced 35.52% in 1-mode, 59.98% in 2-mode and 72.72% in 3-mode shaped response.

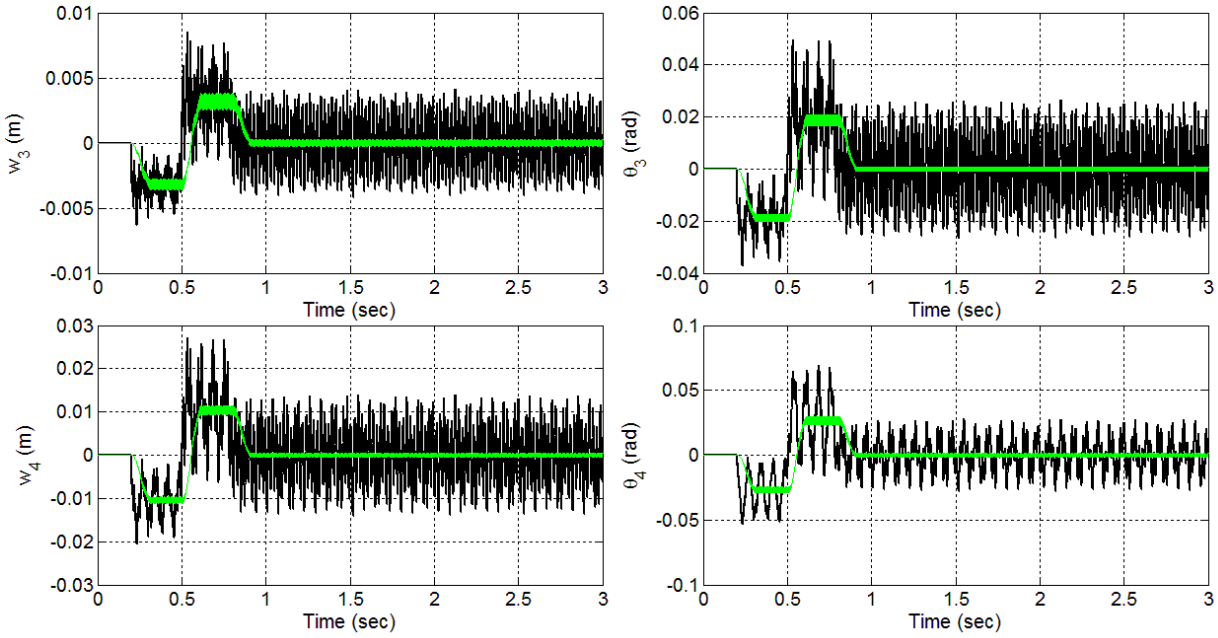

Fig. 5.9: Comparison of bang-bang vs 3-mode shaped response of the single-link flexible manipulator for 3 elements in terms of elastic deflections and angular displacements.

With 3 modes, the elastic deflections and angular displacements are reduced much better with the fine shaped signal. From the Fig. 5.9, in case of elastic deflection w_3, the maximum deflection has been reduced from 0.008497 *m* to 0.003806 *m* which is 0.004328 *m* in case of shaped response of 2 modes. The respective maximum angular position of the link element is 0.0209 *rad* for shaped response. In case of elastic deflection w_4, the maximum deflection of the shaped response reduced from 0.0272 *m* to 0.0115 *m*. For the respective angular deflection θ_4, the maximum deflection is 0.030 *rad*, reduced by 56.8% from unshaped response.

5.3 Vibration Suppression using Proportional-Derivative Control

The vibrations in the flexible manipulator can be controlled better by using closed-loop controls. In this section, the results from proportional-derivative control scheme are discussed. The control scheme is implemented on the dynamic model already developed in the Chapter 3 and results for suppressed vibration levels are discussed.

The desired trajectory that manipulator has to follow is $\pm 80°$. The vibrations of the flexible system are suppressed by a closed-loop scheme i.e. PD control. The system is passed 4 impulses and results are presented for first three different modes of vibration because these three modes are dominant and show characteristic behavior of the flexible system. The simulation is run for 12 *sec* for 1st mode value of 13.31 *Hz* and the following results are obtained.

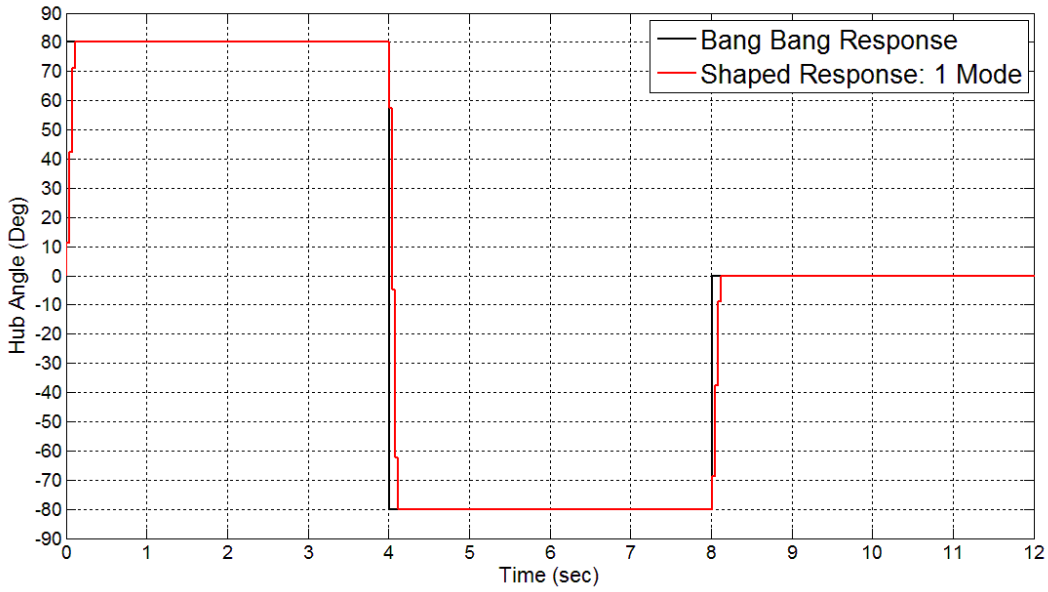

Fig. 5.10: Bang bang response vs 1 mode shaped response

From the Fig. 5.10, it is can be noted that how the response is shaped and used to achieve the first positive amplitude of 80 *deg* hub angle input profile. This trajectory is very difficult to achieve for the manipulator in zero time. So, it is shaped with first mode of vibration as shown. Thus, first positive the amplitude of 80 *deg* is achieved by the manipulator in 0.11 *sec*.

In this simulation, both input shaping and PD control are implemented simultaneously. For the three mode cases, i.e. 13.31 *Hz*, 35.11 *Hz* and 65.76 *Hz*, the desired shaper parameters are

$$\begin{bmatrix} A \\ t \end{bmatrix} = \begin{bmatrix} 0.1103 & 0.1039 & 0.0978 \\ 0.1119 & 0.0423 & 0.0228 \end{bmatrix} \tag{5.2}$$

The PD control law is given as

$$U(s) = A_c \left[K_P \left\{ \theta_{ds}(s) - \theta(s) \right\} - K_V s\theta(s) \right] \tag{5.3}$$

The gains of PD control law are chosen as

$$\begin{aligned} A_c &= 0.7 \\ K_V &= 2.25 \\ K_P &= 3 \end{aligned} \tag{5.4}$$

From the Fig. 5.11, it is can be seen that the hub angle of +80 *deg* and end point displacement of 1.25 *m* is achieved in about 1.8 *sec* and 2.0 *sec* respectively. The figure shows that shaped response moved minimum distance and hub angle to achieve desired position and angle better than bang-bang response. The end point residual of the shaped response from the bang-bang response is reduced by 34.92%. The maximum velocity achieved by the hub is 80.48 *deg/s*. There is very little difference between hub velocities of the unshaped and shaped response. However, the vibrations are suppressed much better in shaped response while achieving this hub velocity.

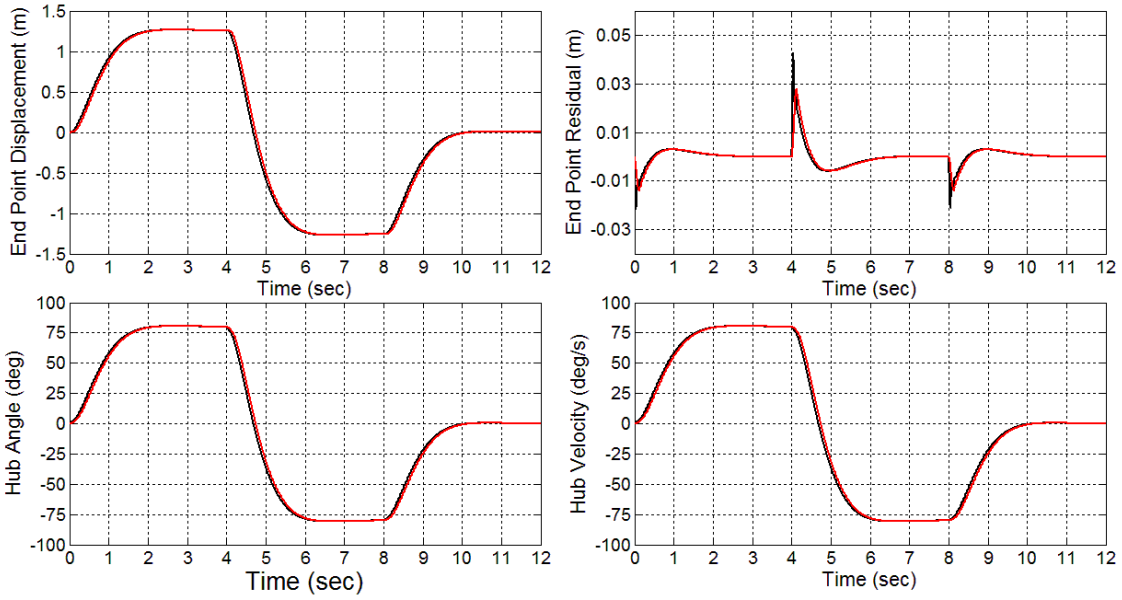

Fig. 5.11: Comparison of Bang-bang response vs 1 mode shaped response of the single-link flexible manipulator for PD control in terms of end-point displacement, end point residual, hub angle and hub velocity.

Now, from the Fig. 5.12, it can be seen that how the structural vibrations in terms of elastic deflections and angular displacements are varied with both response. For the elastic deflection w_3, the deflection in the manipulator is reduced by 25.39% from the bang-bang response. The respective angular displacements θ_3, the unshaped response reduced angular displacement by 28%. In case of elastic deflection w_4, the deflection is decreased by 30.85% where the angular displacement θ_3 is also reduced by 36.83% from the unshaped response.

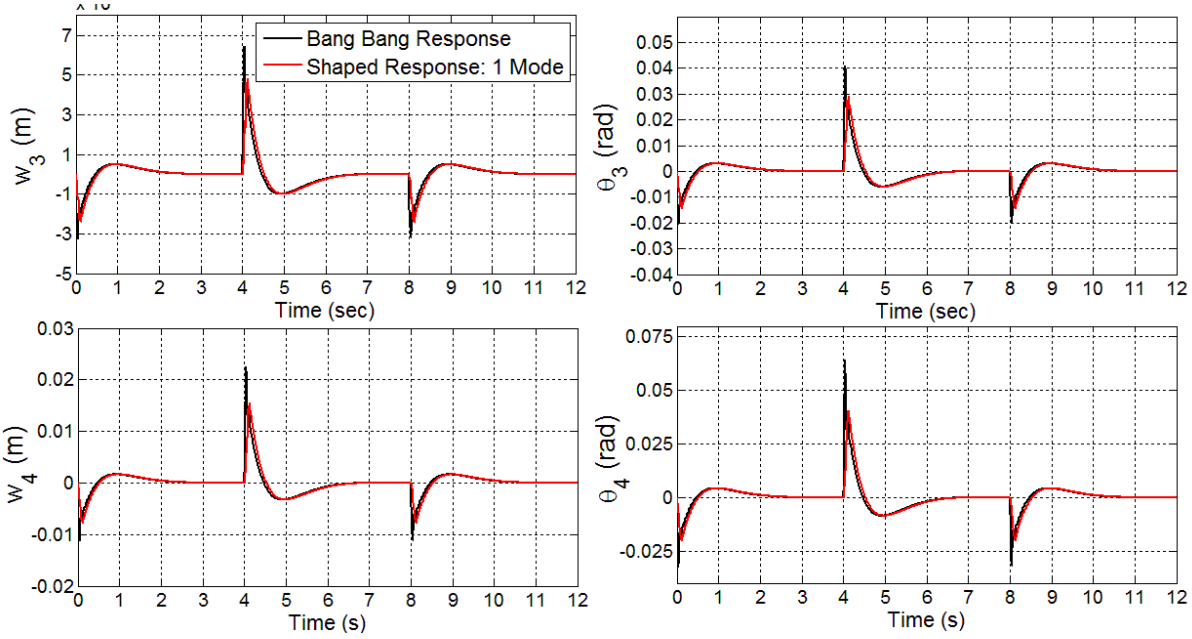

Fig. 5.12: Comparison of bang-bang vs 1-mode shaped response of the single-link flexible manipulator in terms of elastic deflections and angular displacements for PD Control

Now, the two modes of frequencies are considered whose values are 13.31 *Hz* and 35.11 *Hz*, obtained from the dynamic model developed previously. For two modes of vibrations, the shaped response is better than 1 mode and bang-bang response. The input hub angle profile for bang-bang response, 1 mode shaped response and 2 mode shaped response is shown in Fig. 5.13. The first positive amplitude of $\pm 80°$ is achieved within 0.154 *sec* very accurately and smoothly. The number of elements considered for 2 mode shaped response are three and number of impulses are 4. The simulation is run for 12 *sec* to represent the response of bang-bang, shaped response of 1 mode and 2 mode.

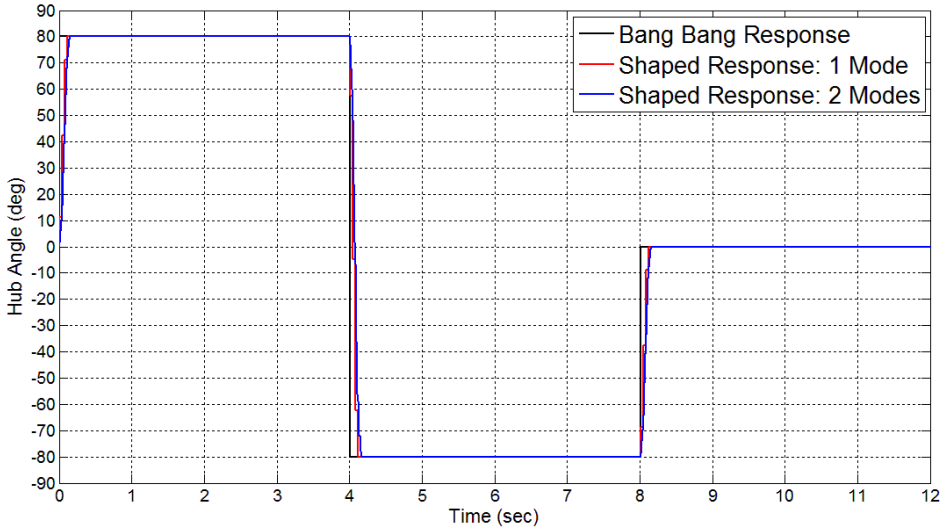

Fig. 5.13: Bang bang response vs shaped response for 1 mode vs shaped response for 2 modes

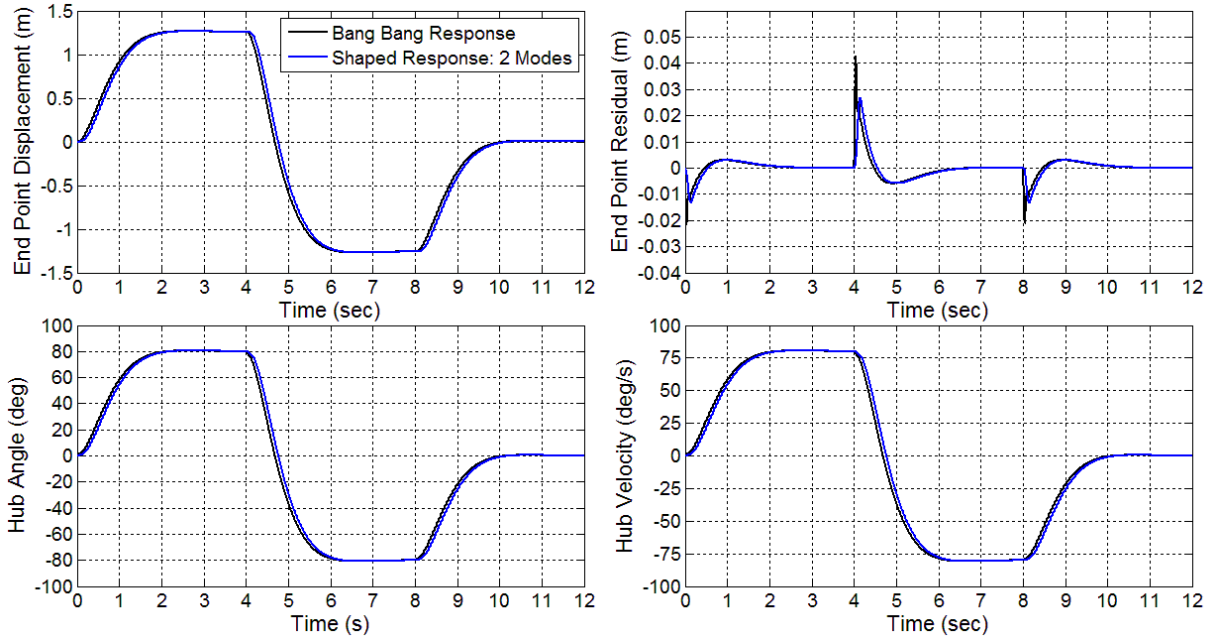

Fig. 5.14: Comparison of Bang-bang response vs 2 mode shaped response of the single-link flexible manipulator for PD control in terms of end-point displacement, end point residual, hub angle and hub velocity.

It can be noted from the Fig. 5.14, the first positive amplitude of 80 *deg* in case of two modes is achieved within 2.25 *sec*. It is 0.02 *sec* more than 1 mode shaped response, thus giving time to manipulator to achieve the required hub angle with minimum vibrations. The end point residual of the 2 mode shaped response is reduced by 37.16% from the bang-bang response. The

maximum velocity achieved by the hub is 80.48 *deg/s* achieved in 2.4 *sec*. Irrespective of minute difference in hub velocity of unshaped and shaped responses, the curves of the shaped response are smoother or vibration free than unshaped response.

Also, it is clear from the Fig. 5.15, the change in modes of vibration has varied the elastic deflections and angular displacements in the manipulator. For elastic deflection w_3, the deflection is reduced by 30.13% from unshaped response and 4.74% less than 2 mode shaped response. The respective angular position of the link is decreased 4.06% and 32.93% from bang-bang and shaped response. For elastic deflection w_4, the deflection peak is reduced by 34% and the respective angular displacement is reduced by 38.88% from the unshaped bang-bang response.

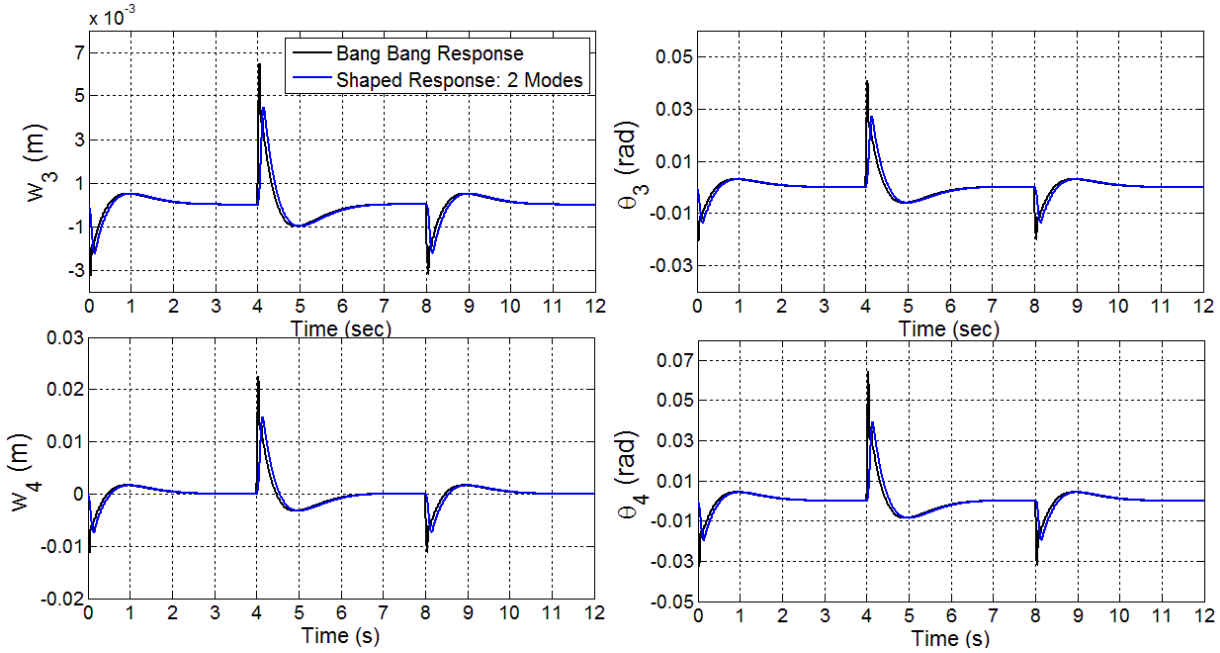

Fig. 5.15: Comparison of bang-bang vs 2-mode shaped response of the single-link flexible manipulator for PD Control in terms of elastic deflections and angular displacements

Now, the PD control is used with three modes of the vibrations. The frequencies of the three modes are 13.31 *Hz*, 35.11 *Hz* and 65.04 *Hz*. The number of impulses used are four, number of elements are three and simulation time is again 12 seconds. The hub angle input profile is shown in the Fig. 5.16. The hub angle of $+80°$ is achieved in 0.1771 *sec*.

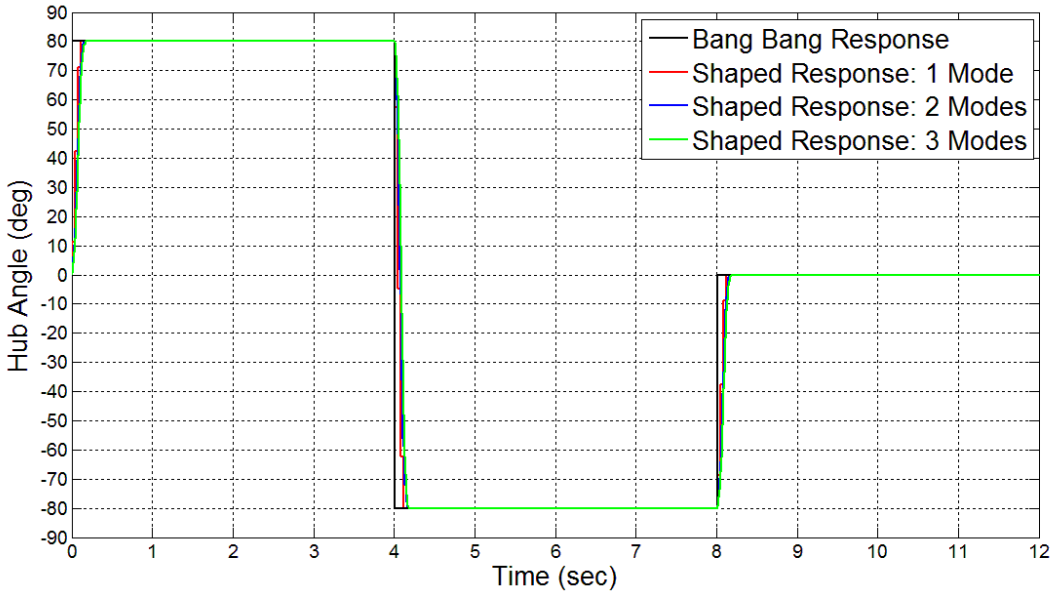

Fig. 5.16: Bang bang response vs shaped response for 1 mode vs 2 modes vs 3 modes

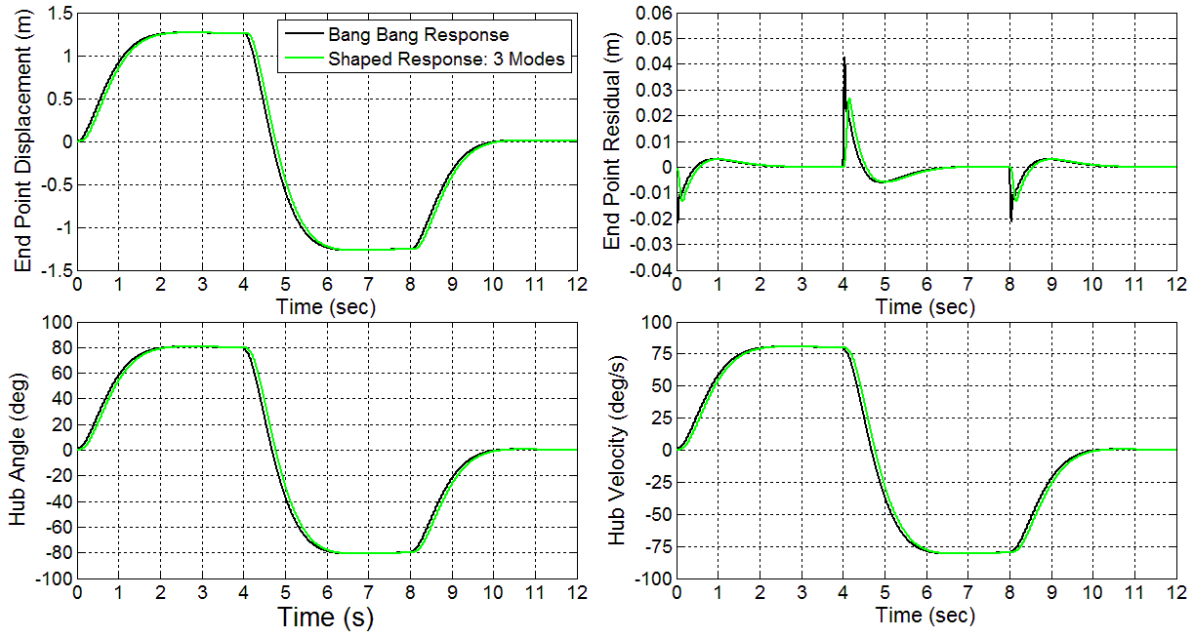

Fig. 5.17: Comparison of Bang-bang response vs 3 mode shaped response of the single-link flexible manipulator for end-point displacement, end point residual, hub angle and hub velocity for PD Control.

It is clear from the Fig. 5.17, the end point residual of the 3 mode shaped response is reduced by 37.81% from the bang-bang response. The first positive amplitude of 80 *deg* hub angle for three modes is achieved within 2.2505 *sec*. It is 0.0005 *sec* more than 2 mode shaped response, thus

giving time to manipulator to achieve the required hub angle with minimum vibrations. The maximum velocity achieved by the hub is 80.48 *deg/s* achieved in 2.26 *sec*. The end point displacement of 1.873 *m* is achieved within 1.225 *sec*.

From the Fig. 5.18, it can be seen that elastic deflections and angular displacements are changed with shaped response. For the elastic deflection w_3, the deflections in the manipulator are reduced by 30.92% from the bang-bang response and 0.44% than 2 mode shaped response. The respective angular displacements θ_3 is reduced 33.34% from unshaped to shaped response. In case of elastic deflection w_4, the deflection is decreased by 35.04% where the respective angular displacement θ_3 is also reduced by 39.41% from the unshaped response.

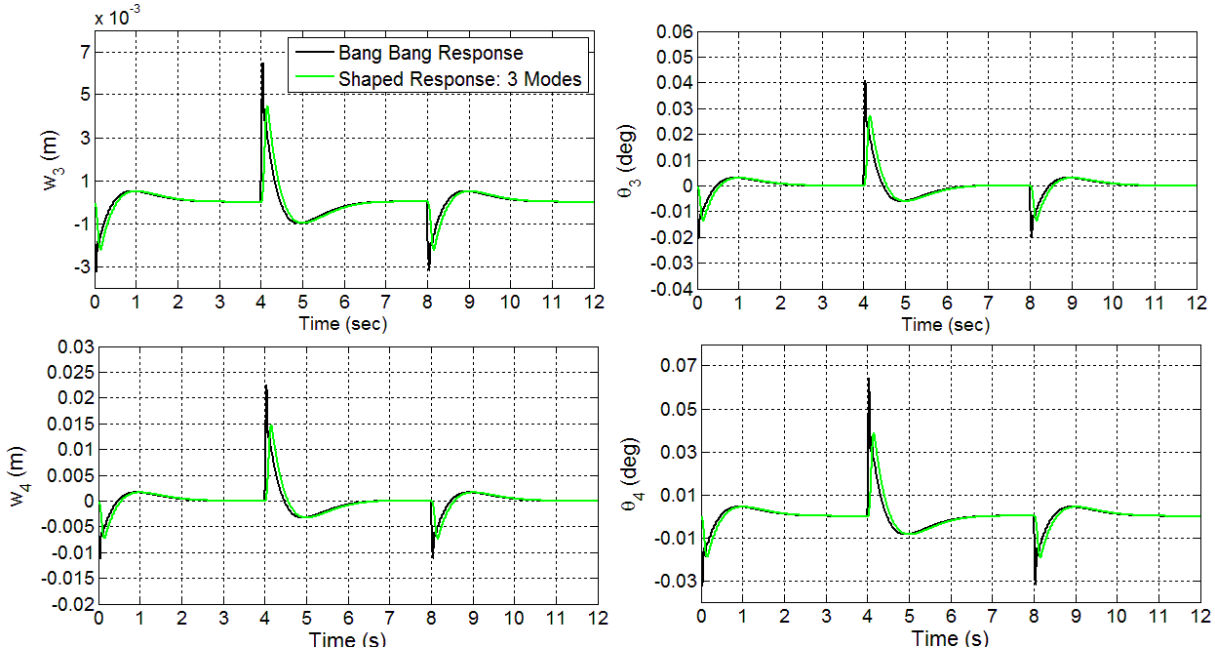

Fig. 5.18: Comparison of bang-bang vs 3-mode shaped response of the single-link flexible manipulator for PD Control in terms of elastic deflections and angular displacements

The percentage reductions in 3 mode shaped response are very little compared to reduction in 2-mode shaped response. It is because the first two modes of the vibration are sufficient enough to suppress the vibration in the manipulator. The third mode frequency is very high, so there is very little reduction in vibration in third mode as discussed above. In the simulation, 3 number of

elements are considered and if the number of elements are increased there may be a possibility that the effect of the third mode can also be seen with a little large difference. For the time being, two modes of vibrations are enough to suppress the vibrations single-link flexible manipulator.

5.4 Summary

In this chapter, the results and simulations related to the vibration suppression of the flexible manipulator are presented. Hybrid control scheme is implemented on the dynamic model of the flexible manipulator and simulation results are presented to show the efficacy of the proposed controller in achieving the desired positional accuracy as well as significant reduction in vibration levels.

CHAPTER 6 CONCLUSION AND FUTURE DIRECTIONS

6.1 Conclusions

In this Chapter, the results obtained from the dynamic model of the flexible manipulator and the simulations for the control of the vibrations in the manipulator are concluded.

1. In the first part of the thesis, an introduction to modeling and control of robot manipulators is presented and how the literature papers included in second part relate to the existing methodologies is presented.

2. Out of various modeling techniques like lumped parameter method, assumed mode method and finite element method, the finite element method is used in the dynamic modeling of the flexible manipulator because complex systems can be easily represented by this technique.

3. The dynamic model developed for the flexible system is validated in frequency domain as well as in time domain.

4. The vibrations of the flexible manipulator can be suppressed easily with command shaping techniques used in closed-loop control schemes.

5. A hybrid controller is developed based on the combination of command shaping and feedback control scheme which suppress the vibrations efficiently.

6. The input shaping control scheme is found to be a better control scheme as compared to the bang-bang torque input control scheme, in terms of positional accuracy and vibration suppression of flexible systems.

6.2 Future Directions

With the experience obtained from the work described in this thesis, several research related questions have built up. It would be interesting to work on following directions in future.

1. The mathematical model for the single-link flexible manipulator is achieved. It can be further extended to multi-link manipulators.

2. The dynamic model and vibration suppression of a planer flexible manipulator has been discussed in previous chapters which can be extended to spatial manipulators also.

3. The analytical approach used to suppress the vibrations of the flexible manipulator can be used in real application systems.

4. The PD control technique is implemented on the flexible manipulator in this thesis. However, other hybrid and optimal control techniques can be implemented on the same dynamic model for vibration level comparisons and better performance of the manipulator.

REFERENCES

[1] http://www.imdl.gatech.edu/currentproj/Flex_Manip/Flex_Manip.html

[2] http://www.emeraldinsight.com/content_images/fig/0490330306015.png

[3] http://www.educationaldimensions.com/eLearn/endoscope/images/smallScope.gif

[4] S. Nicosia, P. Tomei and A. Tornambe, "Dynamic modeling of flexible robot manipulator", Proceedings of 1986 IEEE International Conference on Robotics and Automation, Vol. 3, pp. 365-372, 1986.

[5] Gordon G. Hasting and Wayne J. Book, "A linear dynamic modeling for flexible robotics manipulator", Control Systems Magazine of IEEE, Vol. 7, Issue 1, pp. 61-64, 1987.

[6] Wayne J. Book, "Modeling, design and control of flexible manipulator arms: A tutorial review", Proceedings of 29th Conference on Decision and Control, pp. 500-506, 1990.

[7] Kenneth L. Hillsley and Stephen Yurkovich, "Vibration control of a two link flexible manipulator", Proceeding of 1991 IEEE International Conference on Robotics and Automation, Vol. 3, pp. 2121-2126, 1991.

[8] S. K. Biswas and R. D. Klafter, "Dynamic modeling and optimal control of flexible robotic manipulator", Proceeding of 1998 IEEE International Conference on Robotics and Automation, Vol. 1, pp. 15-20, 1998.

[9] Mehrdad Farid and Stanislaw A. Lukasiewicz, "Dynamic modeling of spatial manipulators with flexible links and joints", Journal of Computers and Structures, Vol. 75, Issue 4, pp. 419–437, 1999.

[10] Everett L. J. and Compere M., "Designing flexible manipulators with the lowest natural frequency nearly independent of position", IEEE Transaction on Robotics and Automation, Vol. 15, No. 4, pp. 605-611, 1999.

[11] V. O. G. Rosado and E. A. O. Yuhara, "Dynamic modeling and simulation of a flexible robotic manipulator", Robotica, Vol. 17, pp. 523-528, 1999.

[12] V. O. G. Rosado, "A planer flexible robotics manipulator", Kybernetes, Vol. 29, pp.787-796, 2000.

[13] Wen Chen, "Dynamic modeling of multi-link flexible robotic manipulators", Computers and Structures, Vol. 79, Issue 2, pp. 183-195, 2000.

[14] M. O. Tokhi, Z. Mohamed and M. H. Shaheed, "Dynamic characterization of a flexible manipulator system", Robotica, Vol. 19, pp. 571-580, 2001.

[15] Z. Mohamed and M. O. Tokhi, "Vibration control of a single link flexible manipulator using command shaping techniques", Proceedings of Institution of Mechanical Engineers, Part I: Journal of Systems and Control Engineering, Vol. 216, pp. 191-210, 2002.

[16] J. M. Martins, Z. Mohamed, M. O. Tokhi, J. Sa da Costa and M.A. Botto, "Approaches for dynamic modeling of flexible manipulator systems", IEEE Proceedings of Control Theory Applications, Vol. 150, No. 4, pp. 401-410, 2003.

[17] Santosha Kumar Dwivedy and Peter Eberhard, "Dynamic analysis of flexible manipulators: A literature review", Mechanism and Machine Theory, Vol. 41, Issue 7, pp.749-777, 2006.

[18] M. Z. MD. Zain, M. O. Tokhi and Z. Mohamed, "Performance of hybrid learning control input shaping for input tracking and vibration suppression of a flexible manipulator", Teknologi, Vol. 44, pp. 41-64, 2006.

[19] William Singhose, “Command Shaping for Flexible Systems: A Review of the First 50 Years”, International Journal Of Precision Engineering And Manufacturing, Vol. 10, No. 4, pp. 153-168, 2009.

[20] http://automation.isa.org/wp-content/uploads/2011/11/Block-diagram-of-a-typical-PID-control-system.gif

[21] http://xplqa30.ieee.org/ielx5/3516/4088960/4088971/html/img/4088971-fig-11-large.gif

[22] Ashish Tiwari, “Modern Control Design with MATLAB and Simulink”,John Wiley & Sons, Ltd., 2006.